

Circadian regulation of Cav1.2 expression by ROR α in the mouse heart

Estelle Personnic¹, Garance Gerard¹, Corinne Poilbout¹, Anton M. Jetten², Ana Maria Gómez¹, Jean-Pierre Benitah¹, Romain Perrier¹

¹Signalling and cardiovascular pathophysiology, UMR-S 1180, Inserm, Université Paris-Saclay, 91400 Orsay, France.

²Cell Biology Section, NIEHS, National Institutes of Health, Research Triangle Park, Durham, NC 27709, USA.

Short title: Cav1.2 circadian regulation

Address for correspondence:

Jean-Pierre Benitah

Calcium Signalling and Cardiovascular Pathophysiology

Inserm UMR-S 1180

Faculty of Pharmacy

Université Paris-Saclay

17 avenue des Sciences

F-91400 ORSAY

France

jean-pierre.benitah@inserm.fr

Subject Codes: Basic Science Research; Cell Signaling/Signal Transduction; Ion Channels/Membrane Transport; Mechanisms

Word count: Abstract 319; Main text 6797 (including references and figure legends); 7 display Figures/Tables

Abstract

Background. In addition to show autonomous beating rhythmicity, the physiological functions of the heart present daily periodic oscillations. Notably the ventricular repolarization itself varies throughout the circadian cycle which was mainly related to the periodic expression of K^+ channels. However, the involvement of the L-type Ca^{2+} channel ($Ca_v1.2$ encoded by *Cacna1c* gene) in these circadian variations remains elusive.

Methods. We used a transgenic mouse model (PCa-luc) that expresses the luciferase reporter under the control of the cardiac *Cacna1c* promoter and analyzed promoter activity by bioluminescent imaging, qPCR, immunoblot, Chromatin immunoprecipitation assay (ChIP) and $Ca_v1.2$ activity.

Results. Under normal 12:12h light-dark cycle, we observed *in vivo* a biphasic diurnal variation of promoter activities peaking at 9 and 19.5 Zeitgeber time (ZT). This was associated with a periodicity of *Cacna1c* mRNA levels preceding 24-h oscillations of $Ca_v1.2$ protein levels in ventricle (with a 1.5 h phase shift) but not in atrial heart tissues. The periodicity of promoter activities and $Ca_v1.2$ proteins, which correlated with biphasic oscillations of L-type Ca^{2+} current conductance, persisted in isolated ventricular cardiomyocytes from PCa-Luc mice over the course of the 24-h cycle, suggesting an endogenous cardiac circadian regulation. Comparison of 24-h temporal patterns of clock gene expressions in ventricles and atrial tissues of the same mice revealed conserved circadian oscillations of the core clock genes except for the retinoid-related orphan receptor α gene (*ROR α*), which remained constant throughout the course of a day in atrial tissues. *In vitro* we found that *ROR α* is recruited to two specific regions on the *Cacna1c* promoter and that incubation with specific *ROR α* inhibitor disrupted 24-h oscillations of ventricular promoter activities and $Ca_v1.2$ protein levels. Similar results were observed for pore forming subunits of the K^+ transient outward currents, $K_v4.2$ and $K_v4.3$.

Conclusions. These findings raise the possibility that the *ROR α* -dependent rhythmic regulation of cardiac $Ca_v1.2$ and $K_v4.2/4.3$ throughout the daily cycle may play an important role in physiopathology of heart function.

Key Words: heart; circadian rhythm; L-type Ca^{2+} channel;

Nonstandard Abbreviations and Acronyms

AMVC adult mouse ventricular cardiomyocytes

BLI: bioluminescence intensity

BMAL1: Brain and muscle ARNT-like protein-1

CACNA1C: Ca^{2+} voltage-gated channel subunit alpha1 C gene

CACNB2: Ca^{2+} voltage-gated channel auxiliary subunit beta 2 gene

CACNA2D1: Ca^{2+} voltage-gated channel auxiliary subunit alpha2delta 1

Cav1.2: Ca^{2+} channel, voltage-dependent, L type, alpha 1C

Cav1.2-SNT: short N-terminal Cav1.2 isoform

ChIP: Chromatin immunoprecipitation assay

CLOCK: Circadian locomotor output cycles kaput

CRY: Cryptochrome

CT: circadian time

DBP: D-site albumin-binding protein

G_{\max} : maximal conductance

I_{CaL} : LTCC currents

Kv4.2/Kv4.3: Pore forming proteins of the K^{+} transient outward channel

KCND2: K^{+} voltage-gated channel subfamily D member 2 gene

KCND3: K^{+} voltage-gated channel subfamily D member 2 gene

KChIP2: Kv channel-interacting protein 2

KCNIP2: K^{+} voltage-gated channel interacting protein 2 gene:

Klf15: Kidney-Enriched Krueppel-Like Factor 15

LD cycle: light-dark cycle

LTCC: L-type Ca^{2+} channel

NFIL3: Nuclear factor interleukin 3 regulated

NR1D1/2: Nuclear receptors REV-ERB α/β gene

NR1F1: Retinoid-related orphan receptor alpha gene

PCa-luc: Transgenic mouse model that expresses the luciferase reporter under the control of the cardiac *Cacna1c* promoter

PER: Period

qPCR: Quantitative polymerase chain reaction

RLU: relative BLI

ROI: Region of interest

ROR α : the retinoid-related orphan receptor α

RORE: ROR response element

SCN: Hypothalamic suprachiasmatic nucleus

SR1078: ROR α agonist

SR3335: ROR α inverse agonist

TF: transcriptional factors

ZT: Zeitgeber time

Introduction

The biological rhythmicity is fundamental to almost all organisms on earth and plays a key role in health and disease. With its regular beats determined by intrinsic electrophysiological properties of the cardiomyocytes, the heart is the main physiological metronome that we are aware of. Moreover, periodical oscillations of the cardiac contractility, metabolism and electrophysiology are observed throughout the daily cycle to ensures the heart to adapt to geophysical cues, physical exertion and food intake fluctuations by adjusting both its electrical activities and mechanical function¹. Notably, it is long-recognized that the cardiac repolarization, independently of heart rate variation, show marked circadian periodicity that predispose to circadian occurrence of ventricular arrhythmias²⁻⁷. Even if sympathovagal tone, as well as others neurohormonal variations, have been considered as major determinants of these circadian patterns, an innate cellular clock mechanism might also be involved. Indeed, these circadian periodicities are maintained in isolated hearts, tissues and even isolated cardiomyocytes⁸⁻¹⁰. All living organisms from prokaryote to eukaryote have developed within cells throughout the body a highly temporal coordinated integrated network of biological clock to temporal coordination and plasticity of internal biological processes. These biological clocks are highly conserved cell-autonomous autoregulatory transcription-translation feedback loops comprising the interlocked activities of a set of basic helix-loop-helix transcriptional factors (TFs¹¹). A first loop is composed of heterodimerized activators (Brain and muscle ARNT-like protein-1, BMAL1 and Circadian locomotor output cycles kaput, CLOCK) that bind E-box response element in the regulatory regions to induce the transcription of their own repressors (Period, PER1/2/3 and Cryptochrome, CRY1/2) in a cycle that repeats itself in approximately 24 h. A reinforcing loop that is controlled by the first one and modulates *BMAL1* transcription, is formed by the activator D-site albumin-binding protein, DBP and the repressor Nuclear factor interleukin 3 regulated, NFIL3 also known as E4BP4 that through D-box response elements regulate the expression of *NR1F1* and *NR1D1/2*, encoding retinoid-related orphan receptor α (ROR α) and the nuclear receptors REV-ERB α/β , respectively. REV-ERB α and ROR α mediate opposing actions to either inhibit or activate *BMAL1* transcription, respectively, via interaction with a ROR response element (RORRE). In addition, the exact functioning of this molecular clock core depends on a growing number of intracellular factors, including kinases and phosphatases that regulate the stability of molecular clock proteins, as well as chromatin and chromatin-modifying complexes, all of which contribute to produce a molecular rhythm. In turn, this core molecular clock regulates

the periodic expression of nearly 50% of all expressed genes in a tissue-specific manner¹². The central clock mechanism is the hypothalamic suprachiasmatic nucleus (SCN), which via neuronal, endocrine, and paracrine signals¹³ synchronizes peripheral tissue own molecular clock. The heart expresses core circadian clock genes in a time sensitive manner^{14, 15}, controlling the circadian expression of ~10% cardiac transcriptome and proteome¹⁶⁻²¹. The importance of the cardiac molecular clock has been emphasized by generating cardiac-specific circadian gene knockout animals^{6, 22-26}. Remarkably, in all of these models the cardiac repolarization is impaired and associated with the development of cardiac hypertrophy, heart failure and arrhythmias. Cardiac repolarization results from a concerted balance of depolarizing inward currents (mainly Ca^{2+} currents) and repolarizing outward currents (mainly K^{+} currents) in ventricular cells. Strong evidences for a circadian pattern of cardiac K^{+} channels have been provided both in rodent and human heart^{19, 23, 24, 27-30}. Only a couple of controversial studies have assessed the circadian variation the ventricular L-type Ca^{2+} channel (LTCC)³¹⁻³⁵, primarily composed of the $\text{Ca}_v1.2$ pore-forming subunit (encoded by *CACNA1C*), $\text{Ca}_v\beta 2$ and $\text{Ca}_v\alpha 2\delta 1$ auxiliary subunits (encoded by *CACNB2* and *CACNA2D1*, respectively)³⁶. However, the interbreeding of circadian gene datasets for transcripts of *CACNA1C*, *CACNB2* and/or *CACNA2D1* in the heart show circadian expression pattern^{16, 17, 19, 21, 30}. Therefore, it is reasonable to hypothesize a circadian regulation of ventricular LTCCs but the underlying mechanism remains elusive.

Herein, we investigated both *in vivo* and *in vitro* whether the cardiac LTCC oscillated daily using a unique transgenic model that expresses the luciferase reporter under the control of the cardiac *Cacna1c* promoter³⁷.

Methods

Full methods are provided in the Supplemental Material.

Results

In vivo diurnal variation of cardiac $\text{Ca}_v1.2$ expression.

To interrogate the diurnal profile of cardiac LTCC expression, we used PCa-luc mice carrying a firefly luciferase gene under the control of cardiac *Cacna1c* rat promoter³⁷. After a 150 $\mu\text{g/g}$ luciferin injection, the noninvasive *in vivo* bioluminescence imaging of anesthetized PCa-luc mouse showed a strong bioluminescence signal in the heart region (Fig.1A). Although in some mice a weaker signal might be also observed in abdomen and thighs regions, this result

illustrated the cardiac specificity of the *Cacna1c* promoter used. Temporal dynamics analysis in same mouse every 3 h starting at ZT0 (lights on 8 a.m.) under normal 12:12h light-dark cycle (LD cycle, Fig.1A) revealed oscillations of bioluminescence intensity (BLI) during 24 h. One might visualize a first late evening peak (inactive light-on period, ZT 9 corresponding to 5 p.m.) and a second peak at early morning (active lights-off period, ZT 21 or 5 a.m.). These experiments were repeated on 9 different 3-month old mice (Fig.1B). Quantitative analysis of the relative BLI (RLU) within the cardiac ROI showed a non-uniform distribution throughout the 24-h cycle ($P_{ANOVA} < 0.05$) with a 3.78 fold changes of BLI over all times. To infer whether *in vivo* *Cacna1c* promoter activity showed periodicity, the data were analyzed using JTK-Cycle³⁸ with period set at 24 h. We found that BLI varied in a periodic manner ($P_{JTK} < 0.05$, phase at 19.5 and peak-to-through amplitude of 34.14%). For visualization of the temporal relationship, data were represented with harmonic cosinor model with 24 h periodicity, amplitude and phase assigned by JTK-Cycle obtained values. This graphical representation exhibits a bimodal daily pattern: a first peak at early morning (active lights-off period, ZT 19.5 or 4 a.m.) and a second smaller peak at late evening (inactive light-on period, ZT 9 corresponding to 5 p.m.).

Taking into account the 1 to 4 h half-life of luciferase *in vivo*³⁹, one might suggest that the observed promoter activity periodicity could be due to luciferase turnover. We then carried out quantitative reverse transcription polymerase chain reaction (RT-qPCR) analyses of *Cacna1c*, *Cacnb2* and *Cacna2d1* mRNAs extracted from ventricular heart tissues of mice kept in LD cycle and collected at 3-h interval during 24 h (4 mice at each time, Fig. 1C to E). We can infer that the mRNA levels fluctuated throughout the day (2.59, 1.48 and 2.19 fold changes for *Cacna1c*, *Cacnb2* and *Cacna2d1*, respectively) showing a diurnal periodicity with a peak-to-through amplitude of 60.22% for *Cacna1c*, 61.12% for *Cacnb2* and 48.06% for *Cacna2d1* and phases at ZT12. The harmonic cosinor waveform is doubled peaked at ZT12 and between ZT21 and 0. Remarkably, we noticed a direct linear correlation between mRNA levels of the main and auxiliary subunits (insets Fig.1D and E) consistent with a coordinated control of their expressions³⁷.

The presence of a transcript does not necessarily imply the presence of a functional protein. Therefore, we examined the temporal profile of the Cav1.2 protein levels in the same ventricular tissue samples used for qPCR analysis. The immunoblot analysis (Fig.1F and G) documented a diurnal periodicity of Cav1.2 protein levels. A 2.99-fold difference by time was observed and a periodicity characterized with a peak-to-through amplitude of 39.36% and a

1.5-h phase shift compared with *Cacna1c* mRNA. With the harmonic cosinor model, a major peak in the dark cycle (ZT15) and a weaker one in the light cycle (between ZT3 and 6) were observed.

These results suggested *in vivo* temporal differences of ventricular Cav1.2 expressions throughout 24 h controlled at the transcriptional level.

In vitro circadian modulation of Cav1.2 expression and activities.

Diurnal variations in ventricular Cav1.2 expressions *in vivo* could be due to nervous, hormonal signals and/or circadian clock intrinsic to the cardiomyocyte. To address whether periodic oscillation of Cav1.2 expression occurs by cell-autonomous mechanisms, we used isolated ventricular cardiomyocytes from 9 PCa-luc mice kept in culture during 24 h. After isolation (at ZT0) and 2 h-plating, the ventricular cardiomyocytes were acutely submitted to 50% serum shock synchronization for 2 h (given the 0 circadian time)⁴⁰, then collected at 3-h intervals during 24 h and stored at -80°C before protein extraction. Figures 2A and B illustrate that periodic luciferase activities and Cav1.2 expressions (in the same samples) persist in isolated ventricular cardiomyocytes with 24-h oscillations. Robust differences were observed over 24-h period (2.05- and 2.57-fold changes for luciferase activities and Cav1.2 protein levels, respectively). JTK-Cycle analysis showed phases at 16.5 and 9 circadian time (CT) and peak-to-through amplitudes of 16.96% and 26.48%, for luciferase activities and Cav1.2 protein levels, respectively. Similar to *in vivo* analysis although of lower amplitude, the *in vitro* temporal relationship of promoter activity peaked at CT6 and 19 whereas Cav1.2 protein levels peaked at CT9 and 21.

To explore the functional consequences of these circadian rhythmicities, we analyzed the temporal pattern of LTCC currents (I_{CaL}) in isolated ventricular cardiomyocytes submitted to the same protocol using whole-cell patch clamp technique. Figure 2C shows examples of the voltage- and time dependent I_{CaL} densities recorded in myocytes at indicated CTs. A large daily double peaked variations at CT9 and 21 were observed. The analysis was conducted on 7 to 15 different myocytes from 8 mice at 3-h interval (± 15 min) during 24 h and current-voltage relationships were fitted with a function combining the Goldman-Hodgkin-Katz equation and the Boltzmann relationship to estimate maximal conductance (G_{max})⁴¹. The data presented in Figure 2B revealed a 1.71-fold oscillation of G_{max} over 24 h. JTK-cycle analysis identified G_{max} periodic variations (phase at CT9 and peak-to-through amplitude of 38.7%) in concordance with Cav1.2 protein expression (Fig.2B), with peaks at CT9 and 21. Moreover

and consistent with coordinated expression of LTCC subunits *in vivo* (Fig.1C and D), neither the time- nor the voltage-dependent properties of I_{CaL} showed variations during 24 h (Table 1).

The *in vitro* persistent periodicity of transcriptional control of ventricular Cav1.2 activity and expression supports the involvement of endogenous cellular clock mechanism.

Absence of diurnal variation of Cav1.2 in atrial heart tissues.

During the *in vivo* analysis of diurnal variation of *Cacna1c* in ventricular tissues, we also collected in the same mice the atrial tissues. Surprisingly, the analysis of mRNA levels of *Cacna1c*, *Cacnb2* and *Cacna2d1* did not show diurnal periodicity in atria (Fig.3).

To analyze the presence of a molecular clock in our samples, we measured by qPCR sequential mRNA levels of major clock components including transcription factors *Bmal1* (Fig.4A), *Clock* (Fig.4B), *Per1* (Fig.4C), *Per2* (Fig.4D), *Cry1* (Fig.4E), *Cry2* (Fig.4F), *Dbp* (Fig.4G), *Nfil3* (Fig.4H), *Nr1d1* (Fig.4I) and *Nr1f1* (Fig.4J) in both ventricular (left panels) and atrial (right panels) tissues collected during 24 h. As previously reported^{16-19, 22, 23, 42}, all components of the circadian clock transcripts were expressed in ventricular and atrial mouse tissues and showed day-night rhythms except *Nr1f1* (encoding for ROR α). In ventricular tissues (Fig.4J left panel), *Nr1f1* mRNA levels showed 1.79-fold variations over all time and periodically fluctuated (phase at CT9 and peak-to-through amplitude of 40.87%) with a temporal cosinor pattern peaking between CT6-9 and CT15-18. In contrast, no significant difference in the level of *Nr1f1* transcript expression were observed during 24-h cycle in atrial tissues (Fig.4J right panel). There were no differences in the level of ROR α protein expression between ventricular and atrial heart tissues, when compared at the same time points (supplemental Fig.1).

These results point out that there is a functional circadian clock in mouse ventricular and atrial tissues and suggested that ROR α could be an important factor responsible for the diurnal rhythm of ventricular LTCC expressions.

ROR α regulates circadian expression of ventricular Cav1.2

To explore mechanism through which the circadian clock regulated periodic expression of Cav1.2 in the ventricles, we first analyzed the temporal patterns of the ROR α protein levels. Consistent with qPCR analysis (Fig.4J), we denoted that ROR α protein levels both *in vivo* (2.69-fold change, Fig. 5A) and *in vitro* (4.63-fold change, Fig.5B) varied periodically

(phases at ZT13.5 and CT12, peak-to-through amplitude of 36.08 and 72.42%, for *in vivo* and *in vitro* respectively) over the course of the 24-h cycle peaking at 7.5 and 18h.

In silico examination of the ~4 kb cardiac promoter region of mouse *Cacna1c* using TFsearch (https://algggen.lsi.upc.es/cgi-bin/promo_v3/promo/promoinit.cgi?dirDB=TF_8.3), revealed 2 canonical consensus binding sites for ROR α : RORE₁^{Cacna1c} TGGCAGGTCA⁻⁸⁴⁸ and RORE₂^{Cacna1c} TGTAAGGTCA⁻¹⁰³⁰ (site locations relative to the transcription start site of *Mus musculus* strain C57BL/6J NC_000072.6:c119200736-119196242). To examine the potential roles of these ROREs in ROR α mediated regulation of *Cacna1c* expression, we conducted ChIP followed by qPCR on mouse ventricular cardiomyocyte freshly isolated at ZT 9 using (n=4 independent cell isolations) using either mouse anti-ROR α 4 antibody²⁶, anti-RNA Polymerase II Antibody (RNA PolII) as positive control or normal Rabbit IgG as negative IP control (Figure 5C). Relative to the IgG, we found ~3-fold enrichment of ROR α on the two ROREs.

We next examined the effect of pharmacological activation and inhibition of ROR α *in vitro*. After serum synchronization, isolated ventricular myocytes from 3 PCa-luc mice were kept in culture in the absence or the presence of either SR1078, a specific ROR α agonist⁴³ or SR3335, a ROR α inverse agonist⁴⁴ and luciferase activities were measured 24 h later. As shown in Fig. 5D, SR1078- (10 μ M, green box) and SR3335-treatment (5 μ M, red box) increased and reduced, respectively, *Cacna1c* promoter activity. In addition, we showed that in presence of 5- μ M SR3335, *Cacna1c* promoter activities (Fig.5E) and Cav1.2 protein levels (Fig.5F) were devoid of any discernable periodicity over the course of the 24-h cycle.

These data indicate that the ventricular Cav1.2 24-h periodic expression is controlled at transcriptional level by ROR α .

ROR α as a major component in control of the diurnal cardiac repolarization periodicity

It has been reported in rodents that the major early repolarizing K⁺ current formed by Kv4.2/4.3 and KChIP2 subunits showed circadian variation of expression^{23, 27}. Even if it has been shown that the Kidney-Enriched Krueppel-Like Factor 15 (Klf15) transcriptionally controls periodic expression of KChIP2, the molecular mechanism controlling Kv4.2/4.3 circadian rhythmicity is still elusive²³. We analyzed by qPCR the diurnal pattern of *Klf15*, *Kcnip2*, *Kcnd2* and *Kcnd3* (encoding Kchip2, Kv4.2 and 4.3, respectively) transcripts in ventricular (Fig.6 left panels) and atrial (Fig.6 right panels) heart tissues of the same mice. Consistent with previous report²³, we observed a periodic expression of *Kcnip2* and *Klf15*

mRNA in both cardiac tissues (Fig.6A and B). However, as shown in Figure 6C and D, the diurnal variations of *Kcnd2* and *3* (2.16- and 2.01-fold change, respectively) observed in ventricles (phase at CT6, peak-to-through amplitude of 64.20 and 53.49%, for *Kcnd2* and *Kcnd3*, respectively) were absent in atrial tissues of the same mice, suggestive of a potential involvement of ROR α . Indeed, in isolated ventricular cardiomyocytes the 2.12-fold variations of Kv4.3 protein levels throughout the 24-h cycle (phase at CT9, peak-to-through amplitude of 44.588%, Fig. 6E) was blunted in the presence of SR3335 (Fig. 6F). The analysis of mouse *Kcnd2* and *Kcnd3* promoters pointed out the presence of several ROREs: RORE^{*Kcnd2*}: AGAAAGGTCA⁻⁹²³ [NM_019697]; RORE^{*Kcnd3*}₁ TGACCTTCTG⁻⁷⁷⁸ and RORE^{*Kcnd3*}₂ TGACCTCAA⁻³⁰⁰⁸ [NM_019931]). ChIP assay (Fig.6 G) showed ~3-fold enrichment for ROR α binding in the RORE^{*Kcnd2*} and RORE^{*Kcnd3*}₂ but no enrichment in the RORE^{*Kcnd3*}₁ regions.

Discussion

Our study shows that the LTCC expression presents diurnal variations and demonstrated the pivotal role of the transcription factor ROR α , as proximal mediator of cardiac biological clock in this circadian regulation, which might have potential pathophysiological consequences.

Even if diurnal pattern of LTCCs have been previously proposed in the heart, the results are somewhat inconsistent. In ventricular cardiomyocytes from Wistar rats, a nocturnal specie, the I_{CaL} measured at two times of the day was higher in active period (ZT15), even though the Cav1.2 mRNA and protein levels did not change^{31, 34}. In ventricular myocytes of diurnal guinea-pig, a *Clock-Bmal1*-dependant circadian variation of Cav1.2 proteins through PI3K-Akt pathway was associated with simultaneous larger I_{CaL} at ZT3 than at ZT15, but without diurnal variations of *Cacna1c* transcripts³⁵. Conversely, Cav1.2 currents, mRNA and protein expressions peaked during the night under the control of Erk- and PI3K-Akt signaling pathways in embryo chick hearts³² but mRNA and protein expressions of Cav1.2 in WT and cardiomyocyte-specific *Clock* mutant mouse heart remained constant throughout the day³³ whereas these pathways have been shown to regulate cardiac LTCCs^{43, 45}. Our results showed both *in vivo* and *in vitro* in a mouse model (Fig. 1 and 2) consistent diurnal variations of cardiac *Cacna1c* promoter during 24-h cycle, leading to similar periodic variations of Cav1.2 transcripts (with a 3-h phase shift) that precede (by 1.5 h) the simultaneous circadian oscillations of Cav1.2 proteins and currents. While several factors could generate such disparities (species, age, sampling interval, *in vivo/in vitro*, culture conditions....), our data

echoed the results of unbiased approaches by microarrays and RNAseq showing circadian expression of LTCC transcripts. Notably, mouse circadian transcriptomic datasets assessed a biphasic circadian pattern of heart *Cacna1c*, *Cacnb2* and /or *Cacna2d1* genes, with one expression peak in the light phase, and a second peak in the dark^{16, 17, 19}, in agreement with our results. Likewise, query of the primate library of diurnal transcriptome revealed that *CACNB2* and *CACNA2D1* genes in heart peaked in the morning²¹. Moreover, a recent analysis by qPCR in failing human ventricular heart tissues³⁰ reported a circadian pattern of *CACNA1C* expression with 54.1% variance ascribed to a 24 h circadian pattern. In addition, a search in database of cardiomyocyte-specific circadian gene knock-out model revealed alterations of LTCC transcript levels^{22, 46, 47}, pointing out a circadian clock gene-dependent regulation.

In contrast to ventricular tissues, the LTCC and *Nr1f1* transcripts failed to oscillate in mouse atrial tissues (Fig. 3 and 4), whereas cyclic variations of other major components of the circadian clock were maintained. Consistent with these results, a human tissue sample database lookup⁴⁸ revealed that *CACNA1C* and *CACNA2D1* gene in heart atrial do not meet criteria for periodicity. This leads us to hypothesize that ROR α was involved in ventricular Cav1.2 periodicity. Indeed, we observed that specific ROR α inverse agonist prevented circadian rhythmicity of both promoter activities and Cav1.2 protein levels. Analyzing the cardiac promoter region of *Cacna1c* we found 2 putative ROREs. ChIP assay showed that ROR α is indeed recruited onto the cardiac *Cacna1c* promoter in mouse ventricular cells. Matching ROREs in the same sequential order were also found in the upstream region of *Cacna1c* orthologues from rat and human (TGGCAGGTCA⁻⁸⁴⁰ and TGGAAGGTCA⁻⁹²⁶ for *Rattus norvegicus* NC_005103.4:c151273977-151269116 and CTTGAGGTCA⁻²⁶⁴⁰ and CGTGAGGTCA⁻³⁸⁹² for *Homo sapiens* NC_000012.12:1965780-1970880) providing strong evidence for similar and specific gene regulation. Similarly, in mouse brain tissue that expressed the short N-terminal Cav1.2 isoform (Cav1.2-SNT) driven by a different promoter³⁷, 4 putative ROREs have been characterized⁴⁹. This study pointed out a repressive Rev-Erb α -dependent circadian rhythmic Cav1.2-SNT expression participating in setting the SCN circadian clock during the late night, but also showed a ROR α -induced Cav1.2 promoter activity. Indeed, ROR α competes with Rev-Erb α for binding of their shared DNA binding elements and their opposing activities are important in the maintenance of the core mammalian circadian clock⁵⁰. Schmutz et al⁴⁹ observed that circadian amplitudes of Cav1.2-SNT expression were only attenuated by the loss of Rev-Erb α , suggestive of potential role of

ROR α . We thus propose ROR α as output mediator of the circadian molecular clock in the Cav1.2 diurnal regulation.

Recently, the function of ROR α in the heart has gained peculiar interest due to its potential cardioprotective role in ischemia/reperfusion, hypertrophy development and diabetic cardiomyopathy, which could also relay melatonin beneficial cardiac effects^{26, 51-53}. However, to the best of our knowledge, ROR α role in cardiac circadian clock has not been investigated. Nevertheless, it has been shown that thyroid status, which impact cardiac repolarization through regulation of K⁺ and Cav1.2 channels⁵⁴, altered the 24-h rhythms in circadian clock, notably of ROR α , in rat heart⁵⁵. As for Cav1.2, we observed that the diurnal oscillations of the pore forming subunits of K⁺ channels (Kv4.2 and 4.3), underlying the cardiac transient K⁺ outward current (I_{to}), were lost in atrial heart tissues (Fig. 6). Analysis of *Mus musculus Kcnd2* promoter found the presence of one RORE in the mouse, which is conserved in rat and human promoters (at position-934 and -391 for *Rattus norvegicus* [NC_051339.1] and for *Homo sapiens* [NM_012281], respectively). For *Kcnd3*, only matching RORE₂^{Kcnd3} are present in rat and human promoter (TGACCTCAGA⁻³²⁸⁸ for *Rattus norvegicus* [NM_0311739] and TGACCTTCCC⁻¹²⁹⁵ for *Homo sapiens* [NM_172198]). Consistently, ROR α bound to RORE^{Kcnd2} and RORE₂^{Kcnd3} but not on RORE₁^{Kcnd3}. Taken together, this suggests a conservative ROR α -dependent mechanism for the circadian control of cardiac repolarization.

Although, changes in I_{to} do not produce much change in ventricular repolarization in humans, it is quite possible that the additive diurnal changes in Cav1.2 expression, could contribute to the production of potentially lethal arrhythmias. Indeed, Cav1.2 current increase and concomitant K⁺ current decrease lead to prolongation of cardiac repolarization, which allows recovery of Cav1.2 inactivation and generation of an inward depolarizing current during repolarization that triggers early after depolarization that might initiate sustained arrhythmias by reentrant mechanisms³⁶. The temporal occurrence of ventricular arrhythmias is known to have the first peak between morning and noon and the second peak in the evening³⁻⁵, which could be related to the increases on Cav1.2 at both subjective light- and dark-times observed herein.

In conclusion, our results uncovered a new circadian ROR α -dependent cardiac repolarization regulatory mechanism that, in addition to neuronal and hormonal influence, could participate to the daily periodic control of cardiac events.

Acknowledgments

The authors thank Catherine Cailleau (Université Paris-Saclay, CNRS, Institut Galien Paris-Saclay) for her assistance with *in vivo* bioluminescence experiments, Patrick Lechene (Université Paris-Saclay, Inserm, Signalling and Cardiovascular Pathophysiology, UMR-S 1180) for his help with R software and the platforms from “Ingénierie et Plateformes au Service de l’Innovation Thérapeutique” University of Paris-Saclay IPSIT: the AnimEX platform (Julie Burlot, Valérie Domergue) for animal care; the ACTAGen platform (Claudine Deloménie) for qPCR; the CIBLOT platform (Delphine Courilleau) for *in vitro* bioluminescence experiments.

Sources of Funding

This study was supported by grants from the French National Institute for Health and Medical Research (INSERM), the Université Paris-Saclay, the French National Agency for Research (grants: ANR-15-CE14-0005, ANR-19-CE-0031-01 and ANR-23-CE-14-0009-02), the National Institutes of Health (grant 2R01HL055438-22) and the European H2020 program MSCA RISE (grant 734931). UMR-S1180 is a member of the Laboratory of Excellence in Research on Medication and Innovative Therapeutics supported by the Agence Nationale de la Recherche (ANR-10-LABX-33) under the program “Investissements d’Avenir” (ANR-11-IDEX-0003-01). AMJ research was supported by the Intramural Research Program of the NIH (ZO1-ES-101585).

Author Contributions

All authors contributed to conception design and interpretation of the data. EP, GG, CP, RP and JPB contributed to acquisition and analysis of the data. AMJ provided antibody. AMG and JPB acquired the financial supports. All authors read, corrected and approved the final article.

References.

1. Zhang J, Chatham JC and Young ME. Circadian Regulation of Cardiac Physiology: Rhythms That Keep the Heart Beating. *Annu Rev Physiol.* 2020;82:79-101.
2. Browne KF, Prystowsky E, Heger JJ, Chilson DA and Zipes DP. Prolongation of the Q-T interval in man during sleep. *Am J Cardiol.* 1983;52:55-9.
3. Muller JE, Ludmer PL, Willich SN, Tofler GH, Aylmer G, Klangos I and Stone PH. Circadian variation in the frequency of sudden cardiac death. *Circulation.* 1987;75:131-8.

4. Arntz HR, Willich SN, Oeff M, Bruggemann T, Stern R, Heinzmann A, Matenaer B and Schroder R. Circadian variation of sudden cardiac death reflects age-related variability in ventricular fibrillation. *Circulation*. 1993;88:2284-9.
5. Englund A, Behrens S, Wegscheider K and Rowland E. Circadian variation of malignant ventricular arrhythmias in patients with ischemic and nonischemic heart disease after cardioverter defibrillator implantation. European 7219 Jewel Investigators. *J Am Coll Cardiol*. 1999;34:1560-8.
6. Hayter EA, Wehrens SMT, Van Dongen HPA, Stangherlin A, Gaddameedhi S, Crooks E, Barron NJ, Venetucci LA, O'Neill JS, Brown TM, Skene DJ, Trafford AW and Bechtold DA. Distinct circadian mechanisms govern cardiac rhythms and susceptibility to arrhythmia. *Nat Commun*. 2021;12:2472.
7. Molnar J, Zhang F, Weiss J, Ehlert FA and Rosenthal JE. Diurnal pattern of QTc interval: how long is prolonged? Possible relation to circadian triggers of cardiovascular events. *J Am Coll Cardiol*. 1996;27:76-83.
8. Tharp GD and Folk GE, Jr. Rhythmic Changes in Rate of the Mammalian Heart and Heart Cells during Prolonged Isolation. *Comp Biochem Physiol*. 1965;14:255-73.
9. Durgan DJ, Hotze MA, Tomlin TM, Egbejimi O, Graveleau C, Abel ED, Shaw CA, Bray MS, Hardin PE and Young ME. The intrinsic circadian clock within the cardiomyocyte. *Am J Physiol Heart Circ Physiol*. 2005;289:H1530-41.
10. Davidson AJ, London B, Block GD and Menaker M. Cardiovascular tissues contain independent circadian clocks. *Clin Exp Hypertens*. 2005;27:307-11.
11. Patke A, Young MW and Axelrod S. Molecular mechanisms and physiological importance of circadian rhythms. *Nat Rev Mol Cell Biol*. 2020;21:67-84.
12. Takahashi JS. Transcriptional architecture of the mammalian circadian clock. *Nat Rev Genet*. 2017;18:164-179.
13. Schibler U, Gotic I, Saini C, Gos P, Curie T, Emmenegger Y, Sinturel F, Gosselin P, Gerber A, Fleury-Olela F, Rando G, Demarque M and Franken P. Clock-Talk: Interactions between Central and Peripheral Circadian Oscillators in Mammals. *Cold Spring Harb Symp Quant Biol*. 2015;80:223-32.
14. Young ME, Razeghi P and Taegtmeyer H. Clock genes in the heart: characterization and attenuation with hypertrophy. *Circ Res*. 2001;88:1142-50.
15. Leibetseder V, Humpeler S, Svoboda M, Schmid D, Thalhammer T, Zuckermann A, Marktl W and Ekmekcioglu C. Clock genes display rhythmic expression in human hearts. *Chronobiol Int*. 2009;26:621-36.

16. Storch KF, Lipan O, Leykin I, Viswanathan N, Davis FC, Wong WH and Weitz CJ. Extensive and divergent circadian gene expression in liver and heart. *Nature*. 2002;417:78-83.
17. Martino T, Arab S, Straume M, Belsham DD, Tata N, Cai F, Liu P, Trivieri M, Ralph M and Sole MJ. Day/night rhythms in gene expression of the normal murine heart. *J Mol Med (Berl)*. 2004;82:256-64.
18. Podobed P, Pyle WG, Ackloo S, Alibhai FJ, Tsimakouridze EV, Ratcliffe WF, Mackay A, Simpson J, Wright DC, Kirby GM, Young ME and Martino TA. The day/night proteome in the murine heart. *Am J Physiol Regul Integr Comp Physiol*. 2014;307:R121-37.
19. Zhang R, Lahens NF, Ballance HI, Hughes ME and Hogenesch JB. A circadian gene expression atlas in mammals: implications for biology and medicine. *Proc Natl Acad Sci U S A*. 2014;111:16219-24.
20. Dierickx P, Vermunt MW, Muraro MJ, Creyghton MP, Doevendans PA, van Oudenaarden A, Geijsen N and Van Laake LW. Circadian networks in human embryonic stem cell-derived cardiomyocytes. *EMBO Rep*. 2017;18:1199-1212.
21. Mure LS, Le HD, Benegiamo G, Chang MW, Rios L, Jillani N, Ngotho M, Kariuki T, Dkhissi-Benyahya O, Cooper HM and Panda S. Diurnal transcriptome atlas of a primate across major neural and peripheral tissues. *Science*. 2018;359.
22. Bray MS, Shaw CA, Moore MW, Garcia RA, Zanquetta MM, Durgan DJ, Jeong WJ, Tsai JY, Bugger H, Zhang D, Rohrwasser A, Rennison JH, Dyck JR, Litwin SE, Hardin PE, Chow CW, Chandler MP, Abel ED and Young ME. Disruption of the circadian clock within the cardiomyocyte influences myocardial contractile function, metabolism, and gene expression. *Am J Physiol Heart Circ Physiol*. 2008;294:H1036-47.
23. Jeyaraj D, Haldar SM, Wan X, McCauley MD, Ripberger JA, Hu K, Lu Y, Eapen BL, Sharma N, Ficker E, Cutler MJ, Gulick J, Sanbe A, Robbins J, Demolombe S, Kondratov RV, Shea SA, Albrecht U, Wehrens XH, Rosenbaum DS and Jain MK. Circadian rhythms govern cardiac repolarization and arrhythmogenesis. *Nature*. 2012;483:96-9.
24. Schroder EA, Burgess DE, Zhang X, Lefta M, Smith JL, Patwardhan A, Bartos DC, Elayi CS, Esser KA and Delisle BP. The cardiomyocyte molecular clock regulates the circadian expression of Kcnh2 and contributes to ventricular repolarization. *Heart Rhythm*. 2015;12:1306-14.
25. Zhao Y, Xu L, Ding S, Lin N, Ji Q, Gao L, Su Y, He B and Pu J. Novel protective role of the circadian nuclear receptor retinoic acid-related orphan receptor-alpha in diabetic cardiomyopathy. *J Pineal Res*. 2017;62.

26. Beak JY, Kang HS, Huang W, Myers PH, Bowles DE, Jetten AM and Jensen BC. The nuclear receptor RORalpha protects against angiotensin II-induced cardiac hypertrophy and heart failure. *Am J Physiol Heart Circ Physiol*. 2019;316:H186-H200.
27. Yamashita T, Sekiguchi A, Iwasaki YK, Sagara K, Iinuma H, Hatano S, Fu LT and Watanabe H. Circadian variation of cardiac K⁺ channel gene expression. *Circulation*. 2003;107:1917-22.
28. Tong M, Watanabe E, Yamamoto N, Nagahata-Ishiguro M, Maemura K, Takeda N, Nagai R and Ozaki Y. Circadian expressions of cardiac ion channel genes in mouse might be associated with the central clock in the SCN but not the peripheral clock in the heart. *Biol Rhythm Res*. 2013;44:519-530.
29. Gottlieb LA, Lubberding A, Larsen AP and Thomsen MB. Circadian rhythm in QT interval is preserved in mice deficient of potassium channel interacting protein 2. *Chronobiol Int*. 2017;34:45-56.
30. McTiernan CF, Lemster BH, Bedi KC, Margulies KB, Moravec CS, Hsieh PN, Shusterman V and Saba S. Circadian Pattern of Ion Channel Gene Expression in Failing Human Hearts. *Circ Arrhythm Electrophysiol*. 2021;14:e009254.
31. Collins HE and Rodrigo GC. Inotropic response of cardiac ventricular myocytes to beta-adrenergic stimulation with isoproterenol exhibits diurnal variation: involvement of nitric oxide. *Circ Res*. 2010;106:1244-52.
32. Ko ML, Shi L, Grushin K, Nigussie F and Ko GY. Circadian profiles in the embryonic chick heart: L-type voltage-gated calcium channels and signaling pathways. *Chronobiol Int*. 2010;27:1673-96.
33. Ko ML, Shi L, Tsai JY, Young ME, Neuendorff N, Earnest DJ and Ko GY. Cardiac-specific mutation of Clock alters the quantitative measurements of physical activities without changing behavioral circadian rhythms. *J Biol Rhythms*. 2011;26:412-22.
34. Collins HE, Turrell HE, Samani NJ and Rodrigo GC. Diurnal variation in excitation-contraction coupling is lost in the adult spontaneously hypertensive rat heart. *J Hypertens*. 2013;31:1214-23.
35. Chen Y, Zhu D, Yuan J, Han Z, Wang Y, Qian Z, Hou X, Wu T and Zou J. CLOCK-BMAL1 regulate the cardiac L-type calcium channel subunit CACNA1C through PI3K-Akt signaling pathway. *Can J Physiol Pharmacol*. 2016;94:1023-32.
36. Benitah JP, Alvarez JL and Gomez AM. L-type Ca²⁺ current in ventricular cardiomyocytes. *J Mol Cell Cardiol*. 2010;48:26-36.

37. Mesquita TR, Auguste G, Falcon D, Ruiz-Hurtado G, Salazar-Enciso R, Sabourin J, Lefebvre F, Viengchareun S, Kobeissy H, Lechene P, Nicolas V, Fernandez-Celis A, Gomez S, Lauton Santos S, Morel E, Rueda A, Lopez-Andres N, Gomez AM, Lombes M and Benitah JP. Specific Activation of the Alternative Cardiac Promoter of *Cacna1c* by the Mineralocorticoid Receptor. *Circ Res*. 2018;122:e49-e61.
38. Hughes ME, Hogenesch JB and Kornacker K. JTK_CYCLE: an efficient nonparametric algorithm for detecting rhythmic components in genome-scale data sets. *J Biol Rhythms*. 2010;25:372-80.
39. Leclerc GM, Boockfor FR, Faught WJ and Frawley LS. Development of a destabilized firefly luciferase enzyme for measurement of gene expression. *Biotechniques*. 2000;29:590-1, 594-6, 598 passim.
40. Balsalobre A, Damiola F and Schibler U. A serum shock induces circadian gene expression in mammalian tissue culture cells. *Cell*. 1998;93:929-37.
41. Benitah JP and Vassort G. Aldosterone upregulates Ca^{2+} current in adult rat cardiomyocytes. *Circ Res*. 1999;85:1139-45.
42. Durgan DJ, Trexler NA, Egbejimi O, McElfresh TA, Suk HY, Petterson LE, Shaw CA, Hardin PE, Bray MS, Chandler MP, Chow CW and Young ME. The circadian clock within the cardiomyocyte is essential for responsiveness of the heart to fatty acids. *J Biol Chem*. 2006;281:24254-69.
43. Al Katat A, Zhao J, Calderone A and Parent L. Sympathetic Stimulation Upregulates the Ca^{2+} Channel Subunit, $\text{Ca}_v1.2$, via the β_1 and ERK 1/2 Pathway in Neonatal Ventricular Cardiomyocytes. *Cells*. 2022;11.
44. Kumar N, Kojetin DJ, Solt LA, Kumar KG, Nuhant P, Duckett DR, Cameron MD, Butler AA, Roush WR, Griffin PR and Burris TP. Identification of SR3335 (ML-176): a synthetic ROR α selective inverse agonist. *ACS Chem Biol*. 2011;6:218-22.
45. Catalucci D, Zhang DH, DeSantiago J, Aimond F, Barbara G, Chemin J, Bonci D, Picht E, Rusconi F, Dalton ND, Peterson KL, Richard S, Bers DM, Brown JH and Condorelli G. Akt regulates L-type Ca^{2+} channel activity by modulating Cav α_1 protein stability. *J Cell Biol*. 2009;184:923-33.
46. Zhang L, Prosdocimo DA, Bai X, Fu C, Zhang R, Campbell F, Liao X, Coller J and Jain MK. KLF15 Establishes the Landscape of Diurnal Expression in the Heart. *Cell Rep*. 2015;13:2368-2375.
47. Dierickx P, Zhu K, Carpenter BJ, Jiang C, Vermunt MW, Xiao Y, Luongo TS, Yamamoto T, Marti-Pamies I, Mia S, Latimer M, Diwan A, Zhao J, Hauck AK, Krusen B,

- Nguyen HCB, Blobel GA, Kelly DP, Pei L, Baur JA, Young ME and Lazar MA. Circadian REV-ERBs repress E4bp4 to activate NAMPT-dependent NAD(+) biosynthesis and sustain cardiac function. *Nat Cardiovasc Res*. 2022;1:45-58.
48. Ruben MD, Wu G, Smith DF, Schmidt RE, Francey LJ, Lee YY, Anafi RC and Hogenesch JB. A database of tissue-specific rhythmically expressed human genes has potential applications in circadian medicine. *Sci Transl Med*. 2018;10.
49. Schmutz I, Chavan R, Ripperger JA, Maywood ES, Langwieser N, Jurik A, Stauffer A, Delorme JE, Moosmang S, Hastings MH, Hofmann F and Albrecht U. A specific role for the REV-ERB α -controlled L-Type Voltage-Gated Calcium Channel CaV1.2 in resetting the circadian clock in the late night. *J Biol Rhythms*. 2014;29:288-98.
50. Sato TK, Panda S, Miraglia LJ, Reyes TM, Rudic RD, McNamara P, Naik KA, FitzGerald GA, Kay SA and Hogenesch JB. A functional genomics strategy reveals Rora as a component of the mammalian circadian clock. *Neuron*. 2004;43:527-37.
51. Yu L, Sun Y, Cheng L, Jin Z, Yang Y, Zhai M, Pei H, Wang X, Zhang H, Meng Q, Zhang Y, Yu S and Duan W. Melatonin receptor-mediated protection against myocardial ischemia/reperfusion injury: role of SIRT1. *J Pineal Res*. 2014;57:228-38.
52. Beak JY, Kang HS, Huang W, Deshmukh R, Hong SJ, Kadakia N, Aghajanian A, Gerrish K, Jetten A and Jensen B. The nuclear receptor ROR α preserves cardiomyocyte mitochondrial function by regulating caveolin-3-mediated mitophagy. *J Biol Chem*. 2021;297:101358.
53. Chen Y, Zhang SP, Gong WW, Zheng YY, Shen JR, Liu X, Gu YH, Shi JH and Meng GL. Novel Therapeutic Potential of Retinoid-Related Orphan Receptor α in Cardiovascular Diseases. *Int J Mol Sci*. 2023;24.
54. Le Bouter S, Demolombe S, Chambellan A, Bellocq C, Aimond F, Toumaniantz G, Lande G, Siavoshian S, Baro I, Pond AL, Nerbonne JM, Leger JJ, Escande D and Charpentier F. Microarray analysis reveals complex remodeling of cardiac ion channel expression with altered thyroid status: relation to cellular and integrated electrophysiology. *Circ Res*. 2003;92:234-42.
55. Peliciari-Garcia RA, Bargi-Souza P, Young ME and Nunes MT. Repercussions of hypo and hyperthyroidism on the heart circadian clock. *Chronobiol Int*. 2018;35:147-159.

Figure legends

Figure 1. Periodic variations of Ca_v1.2 expression in the mouse heart ventricle. **A.** Bioluminescence images of a PCa-luc mouse recorded at 3-h interval during 24 h from 0 Zeitgeber times (ZT) corresponding to light-on at 8 a.m. The color scale shows relative signal intensity or radiance (expressed in p/sec/cm²/sr), red being the most intense and blue the least intense. **B.** Temporal pattern of heart luciferase activities expressed as relative light units (RLU) of 9 PCa-luc mice. For each mouse at each time point, the total bioluminescence intensity counted for 16 min in the heart region of interest (ROI) were quantified, corrected from the background in the abdomen ROI and normalized to the mean. **C to D.** Time-dependent variations of *Cacna1c* (**C**), *Cacnb2* (**D**) and *Cacna2d1* (**E**) mRNA levels in mouse ventricular tissues. At each time point, tissues were collected on 4 mice (8 at ZT 0) and the relative mRNA levels of each transcript were normalized to the quantity RPL-32 housekeeping gene (ΔCq) and to the mean over all time ($\Delta\Delta Cq$). The fold of change $2^{-\Delta\Delta Cq}$ are expressed as %. Insets in **D** and **E**, represent the fold of change of *Cacnb2* and *Cacna2d1* transcripts, respectively, in function of fold of change *Cacna1c* mRNA in each tissue; the linear fit curves (line in red and 95% confidence level in light red) with correlation Person's coefficients are represented. **F.** Immunoblot with Ca_v1.2 antibody and corresponding total proteins fluorescent staining (TPS) in ventricular heart tissues from different mice collected at 3-h interval during 24 h. **G.** Time series of Ca_v1.2 expression ratios normalized by TPS and mean of each gel in ventricular tissues from mouse heart (n=4 to 8 for each time points). Immunoblots were analyzed by using ImageJ. In **B**, **C**, **D**, **E** and **G** the results of analysis with a non-parametric one-way ANOVA (with repeated measure in B) after Aligned Rank Transform procedure with ARTool R package (P_{ANOVA}) and with JTK-Cycle (P_{JTK}) after being adjusted with Benjamini and Hochberg method are shown and the red lines represent the harmonic cosinor curves. For all the experiments, mice are maintained under normal 12:12h light-dark cycle, the time of light-off is shown in gray.

Figure 2. Temporal pattern of Ca_v1.2 in isolated adult ventricular cardiomyocytes. **A.** Circadian fluctuation of luciferase activities (RLU) in cellular homogenates from isolated adult PCa-luc mouse ventricular cardiomyocytes (AMVC) maintained in culture during 24 h and sampled at 3-h interval after 50% serum shock synchronization (O Circadian time, CT0).

At each time point, the measured BLI per μg of protein are expressed as the ratio of mean in each culture ($n=9$). **B.** $\text{Ca}_v1.2$ immunoblot and TPS of AMVC from the same PCa-luc mouse collected at indicated time (upper panel) and cumulative data (lower panel) from the same samples as in A. Quantification are done as in Figure 1. **C.** I_{CaL} density traces recorded in different AMVCs maintained in culture during indicated time after serum shock synchronization (CT0). I_{CaL} amplitudes were measured and normalized to cell capacitance. **D.** 24-h temporal pattern of maximal conductance of I_{CaL} (G_{max} , $n=9$ to 15 cells per time points). AMVCs were treated with a 2-h serum shock, then I_{CaL} were recorded every $3 \text{ h} \pm 15 \text{ min}$ over a 24-h period. The adjusted p-values (from non-parametric ANOVA, P_{ANOVA} and JTK-Cycle, P_{JTK}) are shown. The data were represented with harmonic cosinor shown as a solid red line.

Figure 3. No change of atrial LTCC transcripts as a function of the time of the day. Expression of *Cacna1c* (A), *Cacnb2* (B) and *Cacna2d1* (C) transcripts in atrial heart tissues of mice maintained under normal 12:12h light-dark cycle and collected at 3-h interval during 24-h cycle ($n=4$ to 8 for each time points). The adjusted p-values (from non-parametric ANOVA, P_{ANOVA} and JTK-Cycle, P_{JTK}) are shown.

Figure 4. Diurnal expression of core clock genes in ventricular and atrial heart tissues at 8 different time points. Expression of clock transcripts across the 24 h cycle in ventricular (left panels) and atrial (right panels) heart tissues from the same mice ($n=4$ to 8 for each time points and group) maintained under normal 12:12h light-dark cycle. The adjusted p-value (from non-parametric ANOVA, P_{ANOVA} and JTK-Cycle, P_{JTK}) are shown. The data are represented with harmonic cosinor when p-values <0.05 and shown as a solid red line.

Figure 5. ROR α mediates circadian changes in ventricular Cav1.2. A and B. Immunoblot with ROR α antibody and TPS (top panels) and quantifications following band densitometry (lower panels) assessing ROR α protein levels in ventricular heart tissues (A, $n=4$ to 8 for each time points) and isolated AMVCs (B, $n=8$ for each time points) collected at 3-h interval during 24 h. C. ChIP assay of immunoprecipitated chromatin from AMVCs (4 different isolations) with a ROR α antibody and quantified qPCR, using a primer sets specific for the putative ROREs in the cardiac *Cacna1c* mouse promoter. Non-immune IgG and DNA immunoprecipitated with RNA polymerase II antibody served as negative and positive controls respectively. D. Luciferase activities of isolated AMVCs from PCa-luc mice treated for 24 h in the absence (control, white box, $n=10$) or in the presence of either ROR α agonist, 10- μM SR1078 (green box, $n=10$), or ROR α inverse agonist, 5- μM SR3335 (red box, $n=10$).

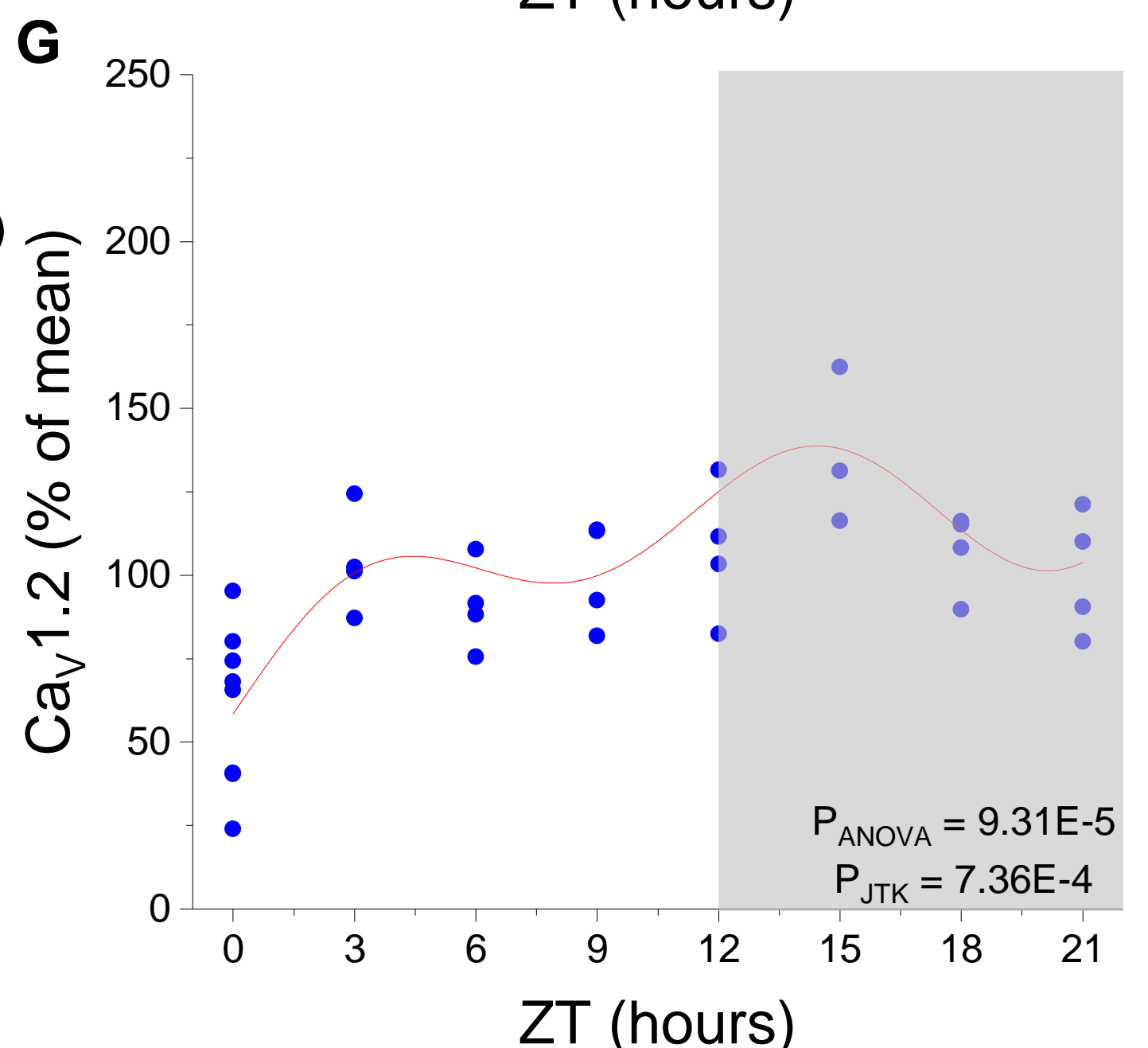
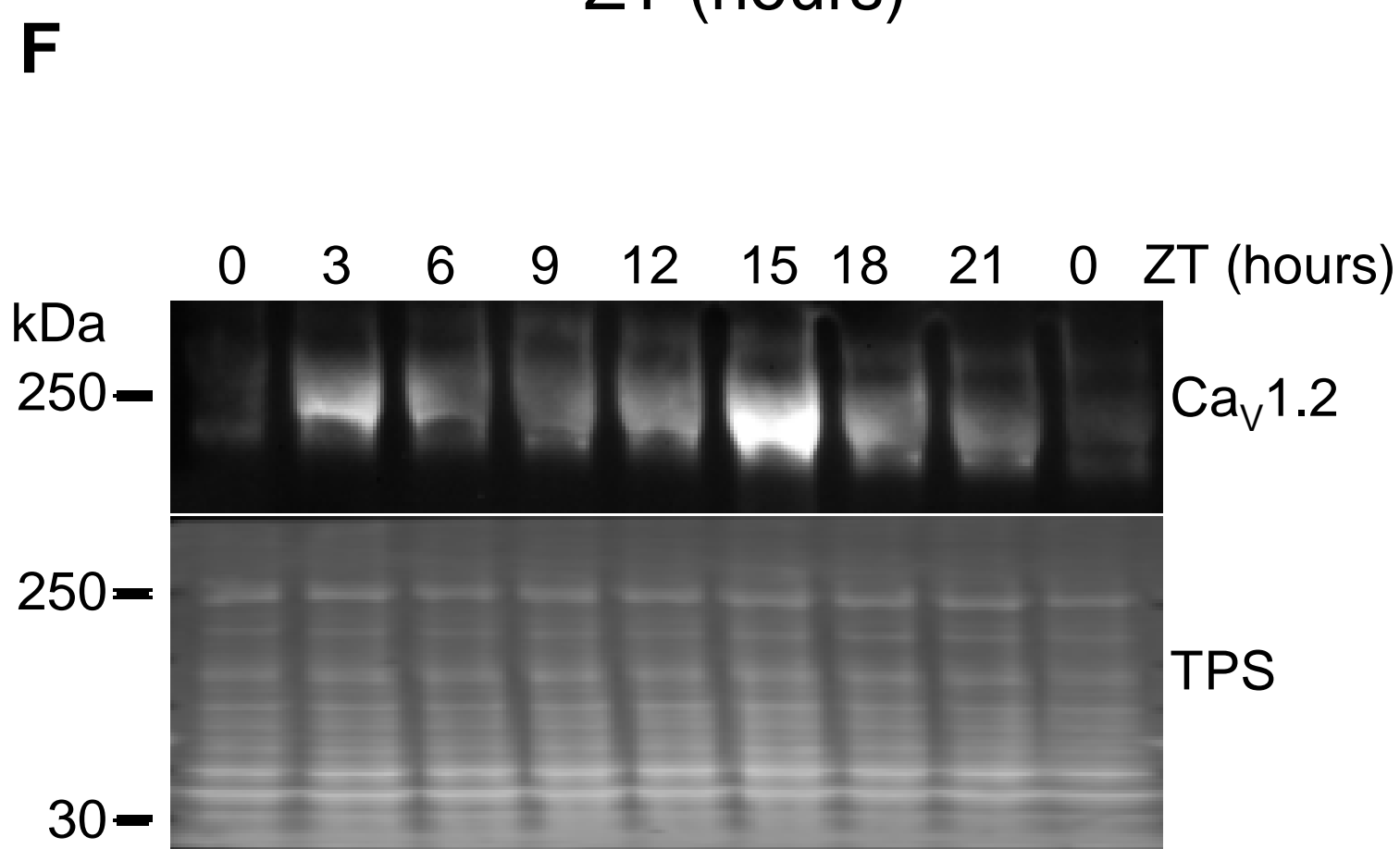
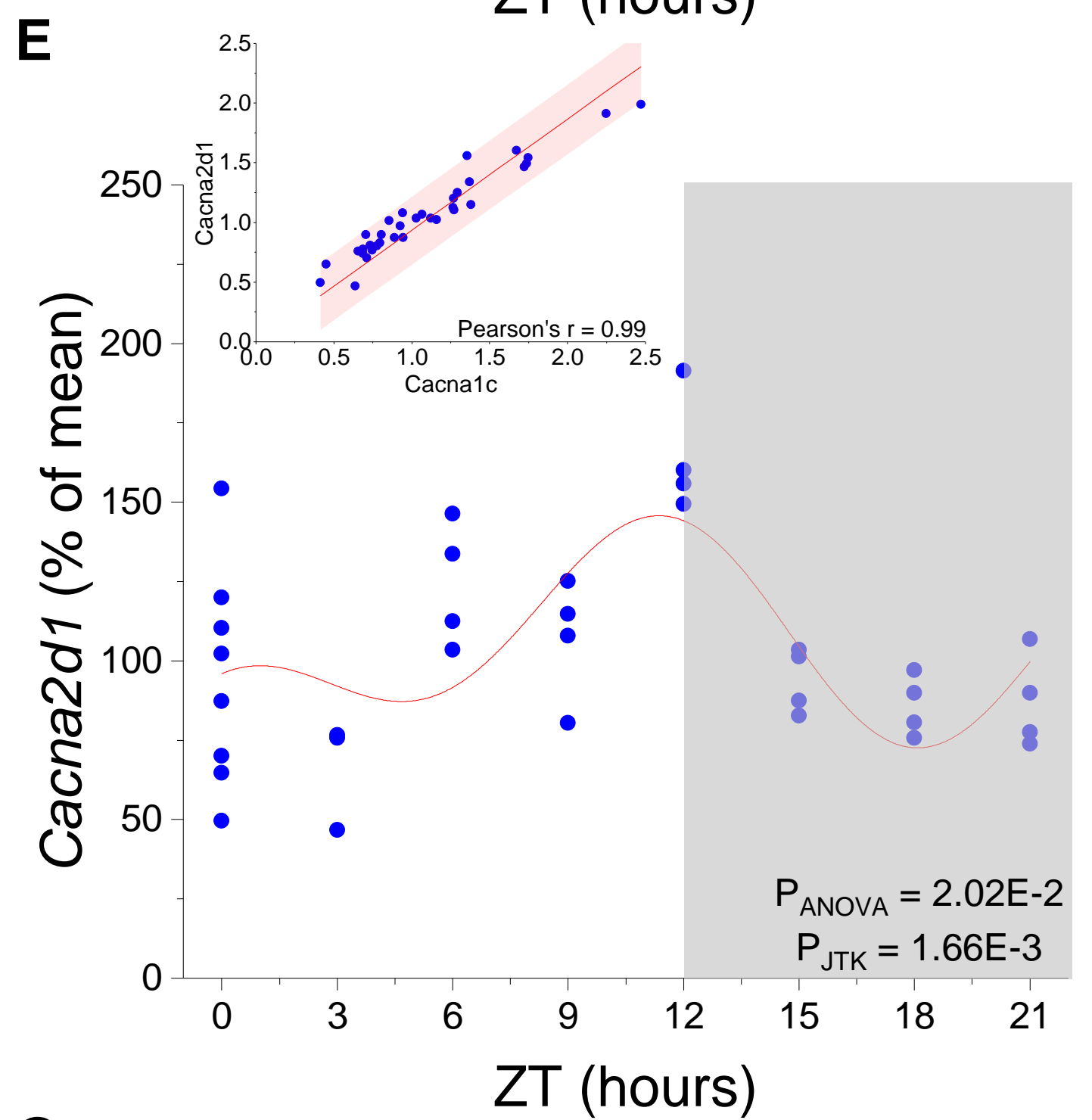
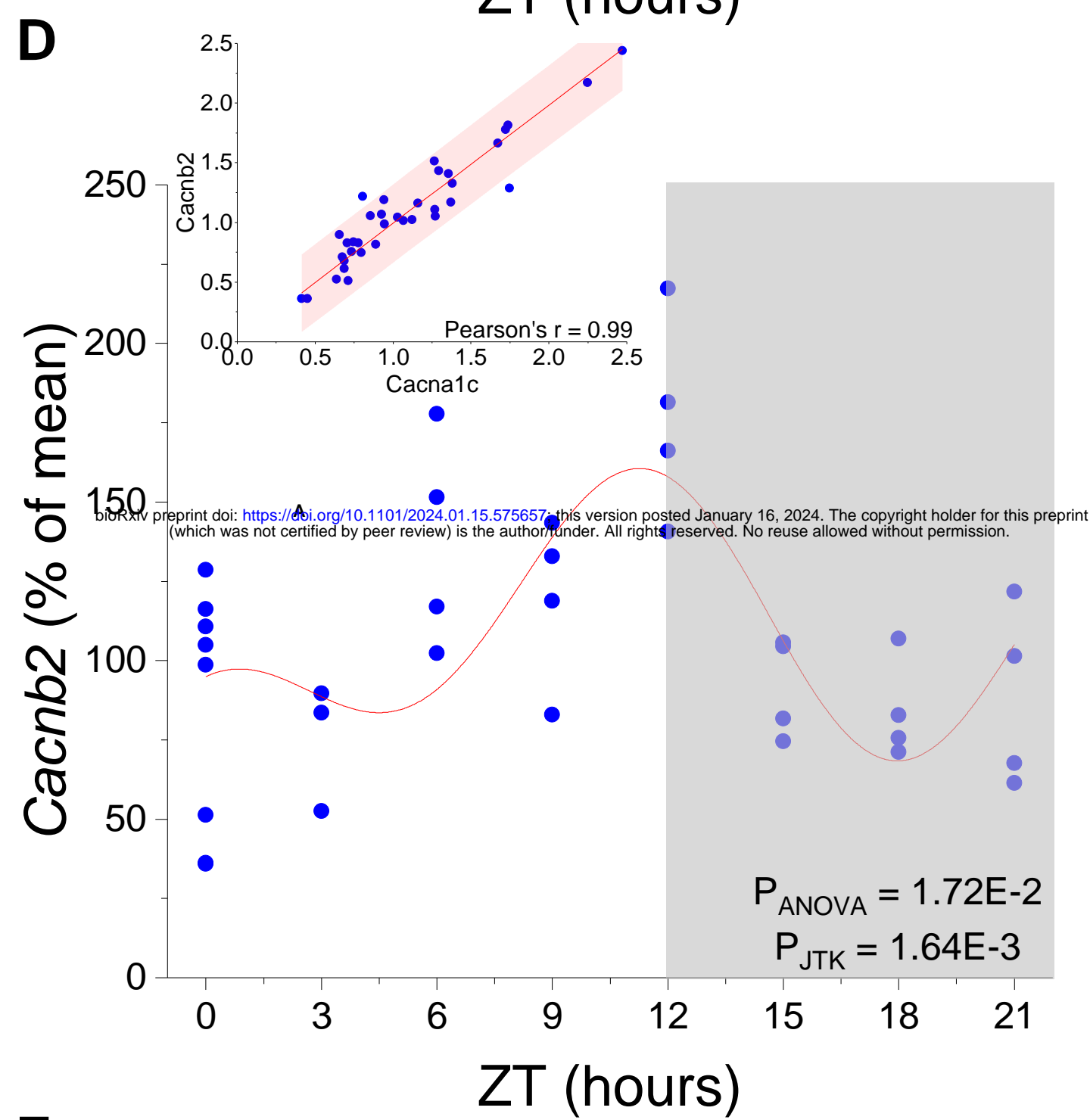
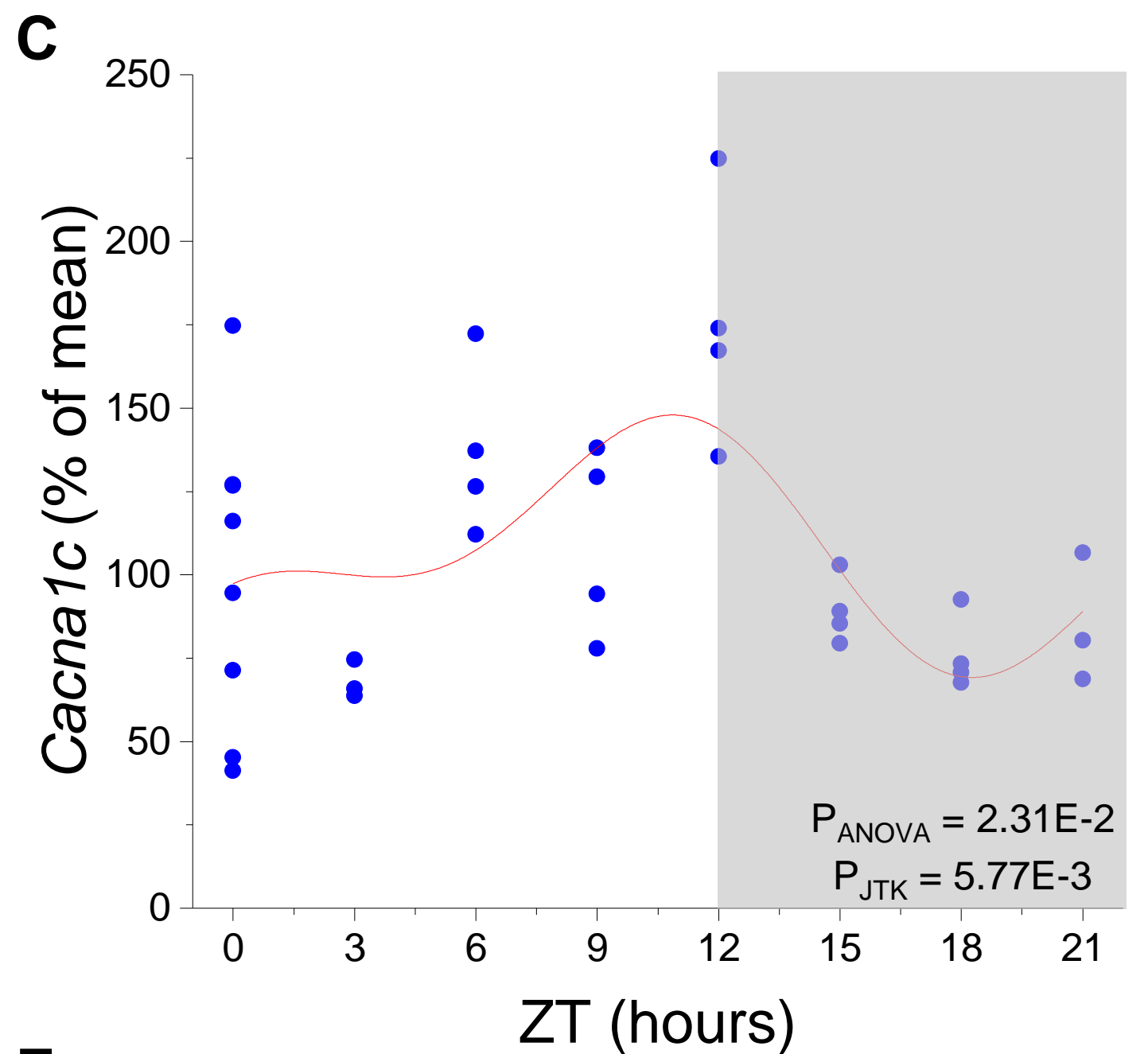
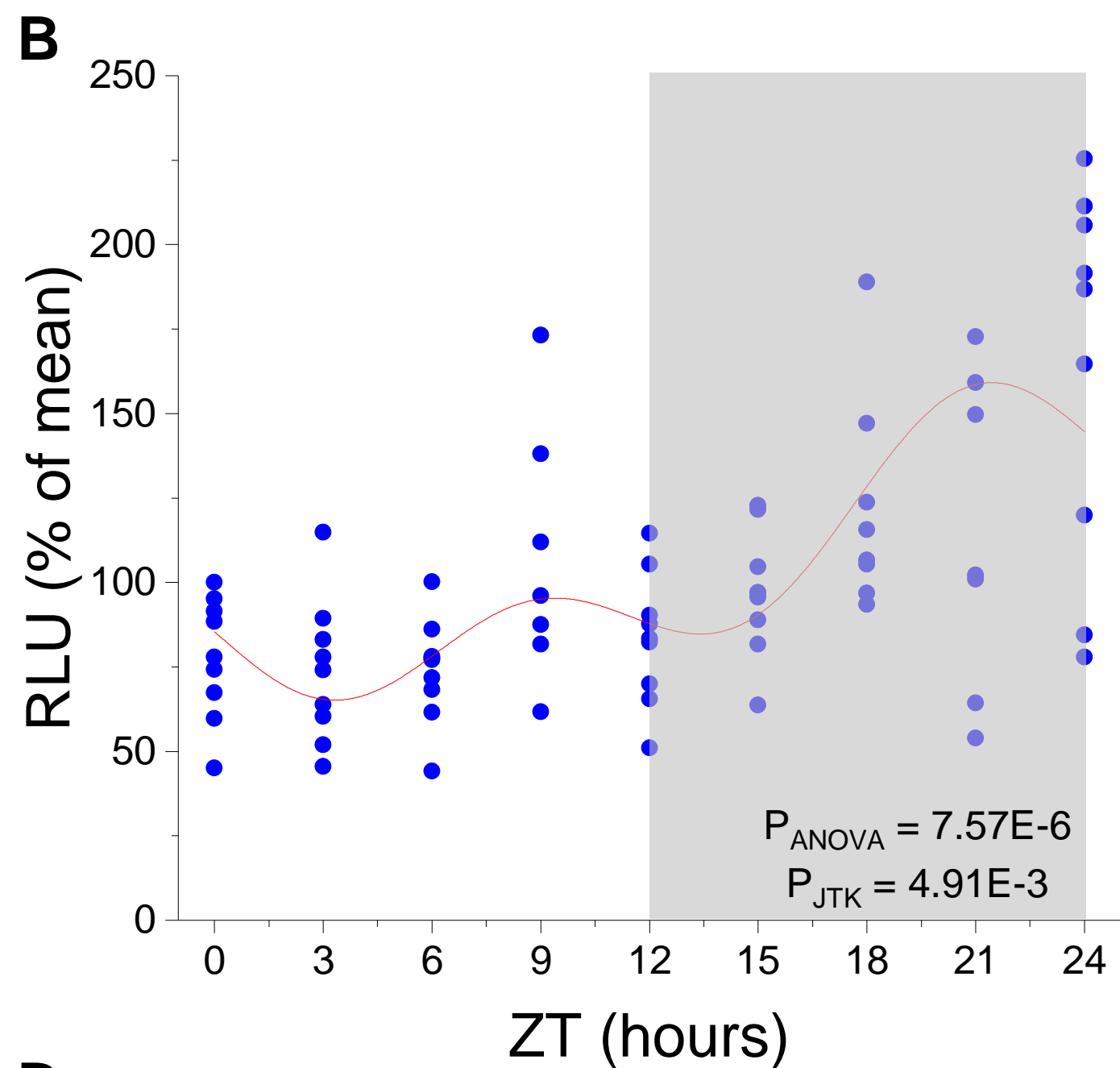
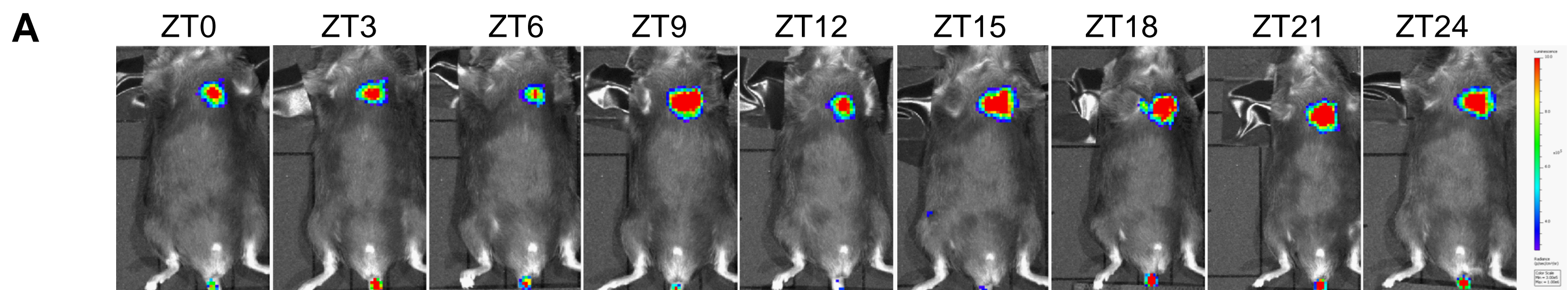
Data are presented as median (line) and 95% confidence interval (box). **E** and **F**. Time-course data of luciferase activities (**E**) and Cav1.2 protein levels (**F**, upper inset showing immunoblot with Cav1.2 antibody and TPS) in AVMCs maintained during 24 h in presence of 5- μ M SR3335 (n=3 for each time points). The adjusted p-value (from non-parametric ANOVA, P_{ANOVA} and JTK-Cycle, P_{JTK}) are shown and overlay of harmonic cosinor models are shown when p-values <0.05.

Figure 6. Potential role of ROR α in mediating diurnal variations in transient K⁺ outward channel transcripts. **A to D.** Expression of *Kcnip2* (**A**), *Klf15* (**B**), *Kcnd2* (**C**) and *Kcnd3* (**D**) transcripts across the 24 h cycle in ventricular (left panels) and atrial (right panels) heart tissues from the same mice (same sample as Fig.1 and 3) maintained under normal 12:12h light-dark cycle. **E** and **F**. Time-course of Kv4.3 protein levels in AVMCs maintained during 24 h in the absence (**E**, n= 8 for each time points) or in the presence of 5- μ M SR3335 (**F**, n= 3 for each time points). Upper insets showing immunoblot with Kv4.3 antibody and TPS. The adjusted p-value (from non-parametric ANOVA, P_{ANOVA} and JTK-Cycle, P_{JTK}) are shown and overlay of harmonic cosinor models are shown when p-values <0.05 and shown as a solid red line. **G.** ChIP assay of immunoprecipitated chromatin from AVMCs (4 different isolations) with a ROR α antibody and quantified qPCR, using a primer sets specific for the putative ROREs in the *Kcnd2* and 3 mouse promoters. Non-immune IgG and DNA immunoprecipitated with RNA polymerase II antibody served as negative and positive controls respectively.

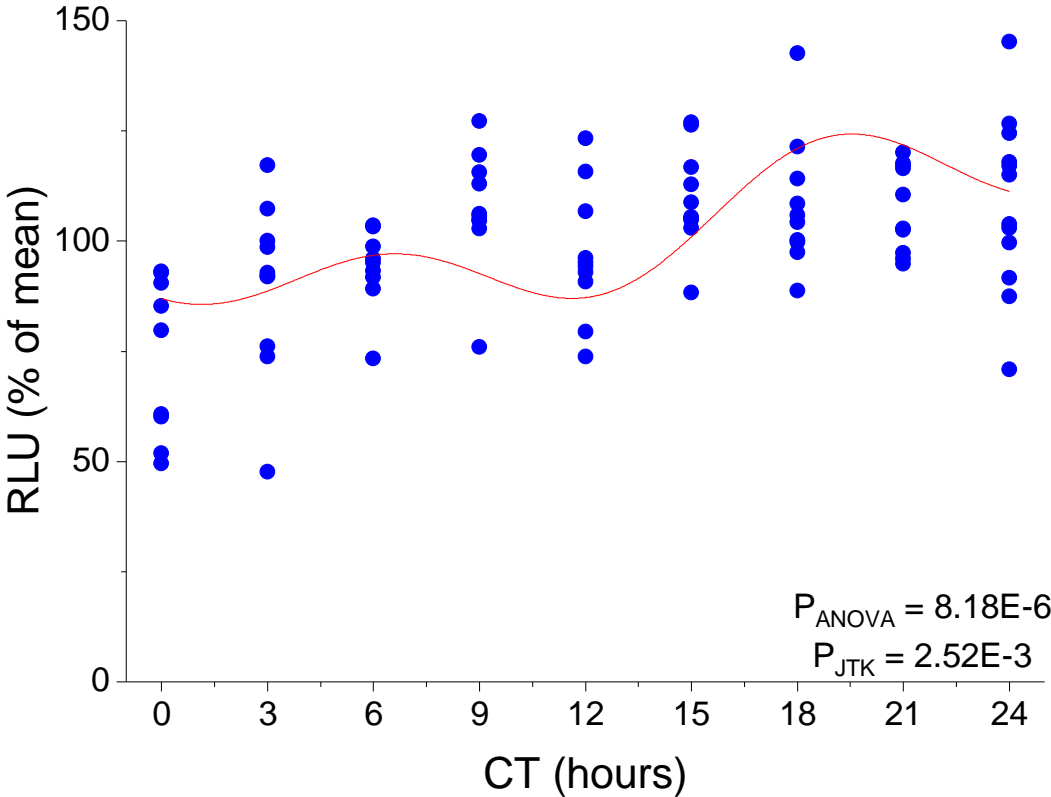
Table 1. Temporal cellular electrophysiology characteristics of isolated ventricular cardiomyocytes.

	n _{cell}	CT0 8	CT3 10	CT6 13	CT9 10	CT12 9	CT15 13	CT18 10	CT21 15	CT24 12	P _{ANOVA}
C _m (pF)		156.67 [135.9,177.4]	147.49 [134.7,169.7]	145.43 [132.4,160.2]	140.90 [97.6,163.3]	150.65 [98.1,220.7]	150.64 [135.1,181.4]	126.07 [120.2,171.1]	102.88 [95.2,144.2]	106.19 [101.7,156.7]	0.155
Activation											
T _{peak} (msec)		8.75 [7.7,12.2]	8.80 [8.3,10.1]	9.20 [8.8, 9.4]	7.80 [7.5, 9.0]	9.00 [8.4, 11.9]	8.20 [7.4, 8.4]	8.65 [7.4, 9.8]	7.70 [7.2, 8.8]	7.40 [6.5, 8.2]	0.245
V ₅₀ (mV)		-9.08 [-11.2, -8.4]	-11.98 [-14.8, -8.3]	-11.87 [-12.4, -9.3]	-10.26 [-11.7, -8.9]	-12.79 [-13.5, 9.5]	-10.65 [-14.1, -8.5]	-10.40 [-1.8, -7.8]	-11.65 [-13.3, -10.2]	-10.39 [-12.0, -8.9]	0.415
k (mV)		-7.35 [-8.2, -6.6]	-5.93 [-7.9, -5.1]	-5.61 [-6.4, -5.4]	-6.21 [-7.7, -5.8]	-5.27 [-6.6, -4.8]	-5.97 [-6.6, -5.3]	-6.09 [-6.9, -5.8]	-5.78 [-6.8, -5.2]	-6.71 [-7.8, -5.4]	0.150
Inactivation											
V ₅₀ (mV)		-23.94 [-30.3, -22.1]	-26.08 [-26.9, -22.4]	-24.05 [-25.3, -23.7]	-23.77 [-25.3, -23.5]	-26.27 [-27.2, -25.2]	-25.70 [-29.2, -24.2]	-24.39 [-25.6, -22.1]	-25.83 [-27.5, -24.4]	-25.89 [-30.5, -22.8]	0.561
k (mV)		6.79 [5.4, 8.5]	5.75 [4.9, 5.9]	5.78 [5.5, 6.4]	6.86 [6.2, 7.2]	5.50 [5.4, 6.1]	5.87 [5.5, 6.3]	6.43 [5.6, 7.8]	6.19 [5.7, 6.9]	7.01 [6.2, 8.3]	0.154
τ _{slow} (msec)		90.14 [83.5, 104.5]	78.52 [70.8, 85.7]	88.36 [80.4, 94.1]	89.62 [78.5, 101.5]	86.59 [84.2, 90.3]	84.22 [76.6, 96.3]	87.32 [79.2, 121.9]	81.73 [75.6, 95.7]	90.96 [84.7, 128.6]	0.433
τ _{fast} (msec)		9.20 [7.1, 10.1]	9.57 [8.9, 11.7]	9.79 [8.4, 11.2]	8.19 [7.1, 9.1]	9.26 [6.6, 10.3]	10.56 [8.1, 11.3]	8.14 [7.3, 9.8]	8.94 [8.1, 10.2]	7.05 [6.8, 9.4]	0.209

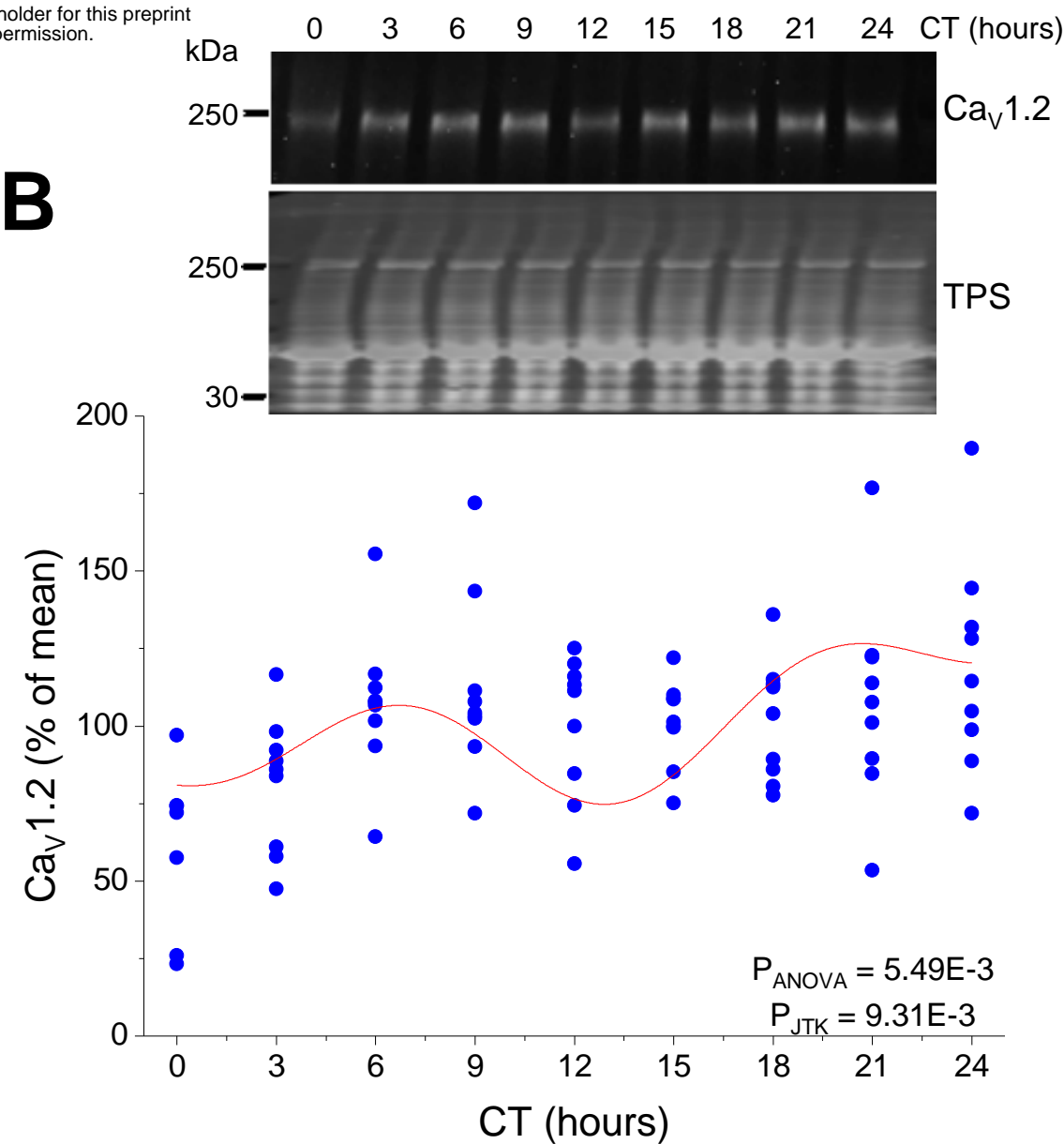
Data are presented as median [95% confidence interval]. n_{cell} is the number of cell analyzed. T_{peak} is the time from the onset of the voltage step to the peak of current at 0 mV, V₅₀ is the potential of half-maximum and k is the slope factor for both activation and inactivation. τ are the time constants of the two components of the time course of inactivation at 0 mV subscripted fast and slow, respectively. P_{ANOVA} are the p values of one-way ANOVA on aligned rank transform data with the ARTool R package.



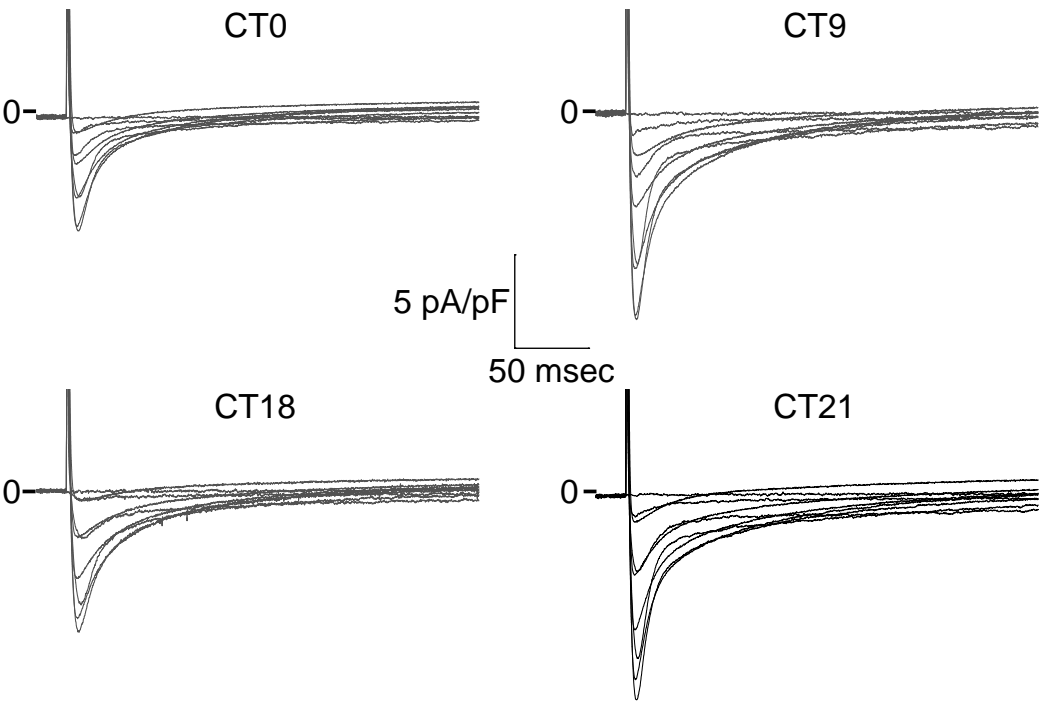
A



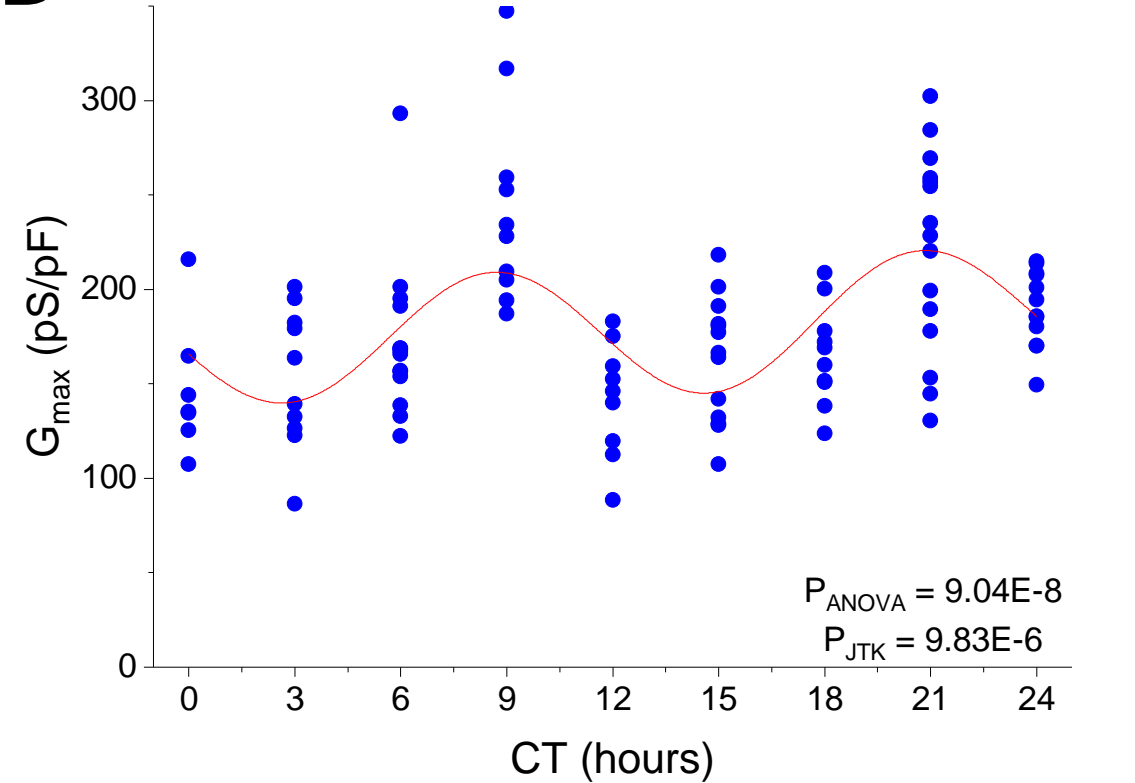
B

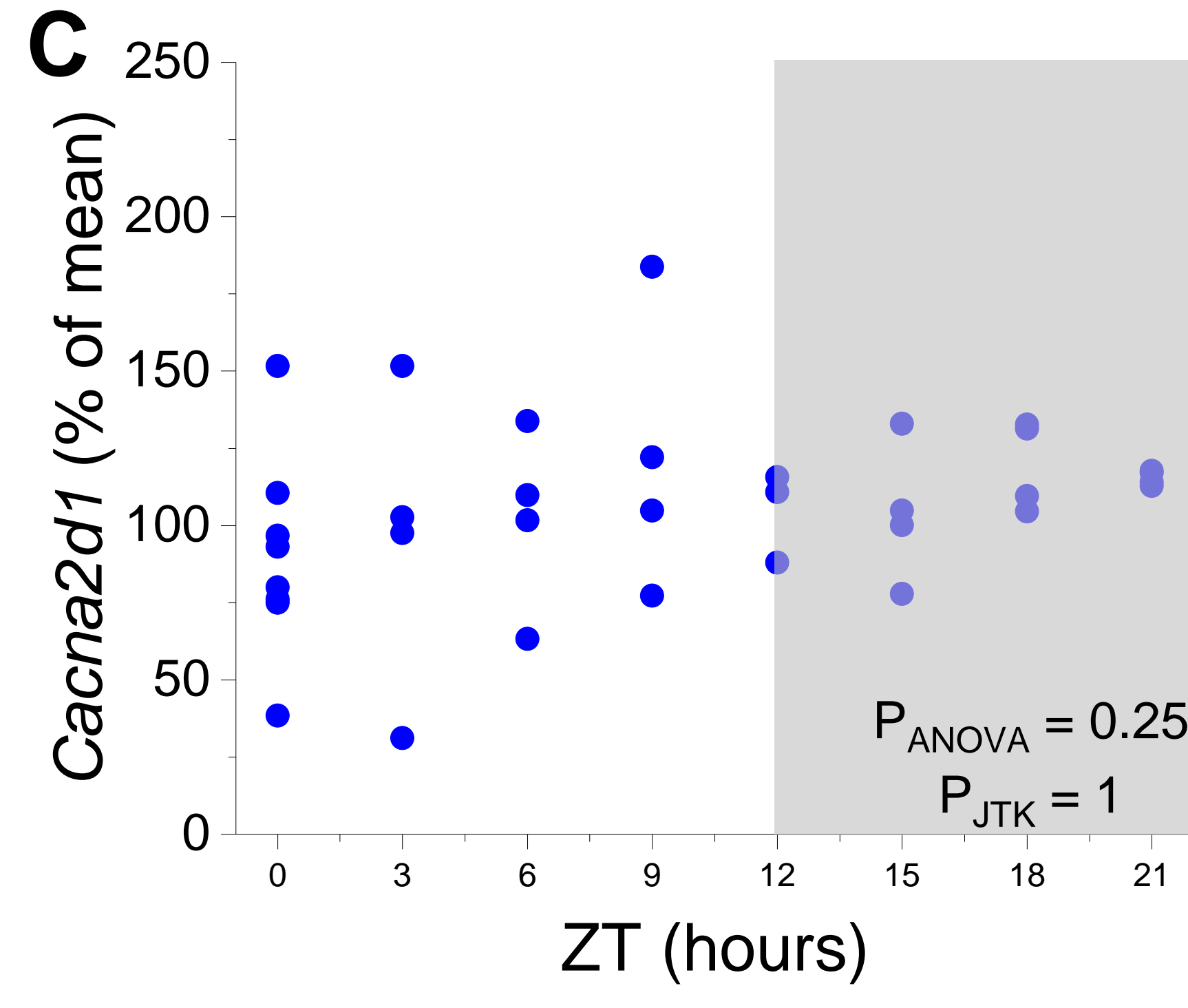
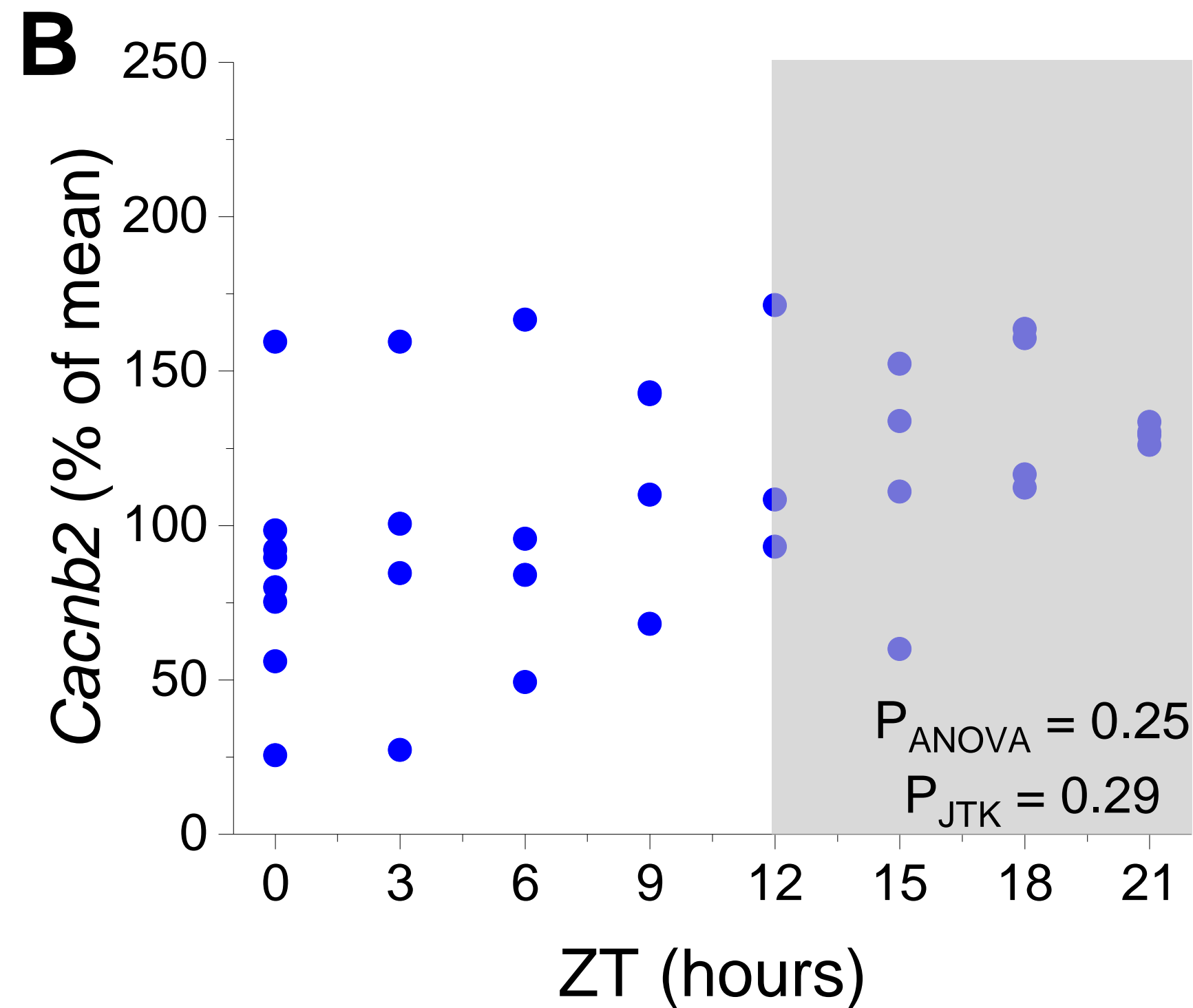
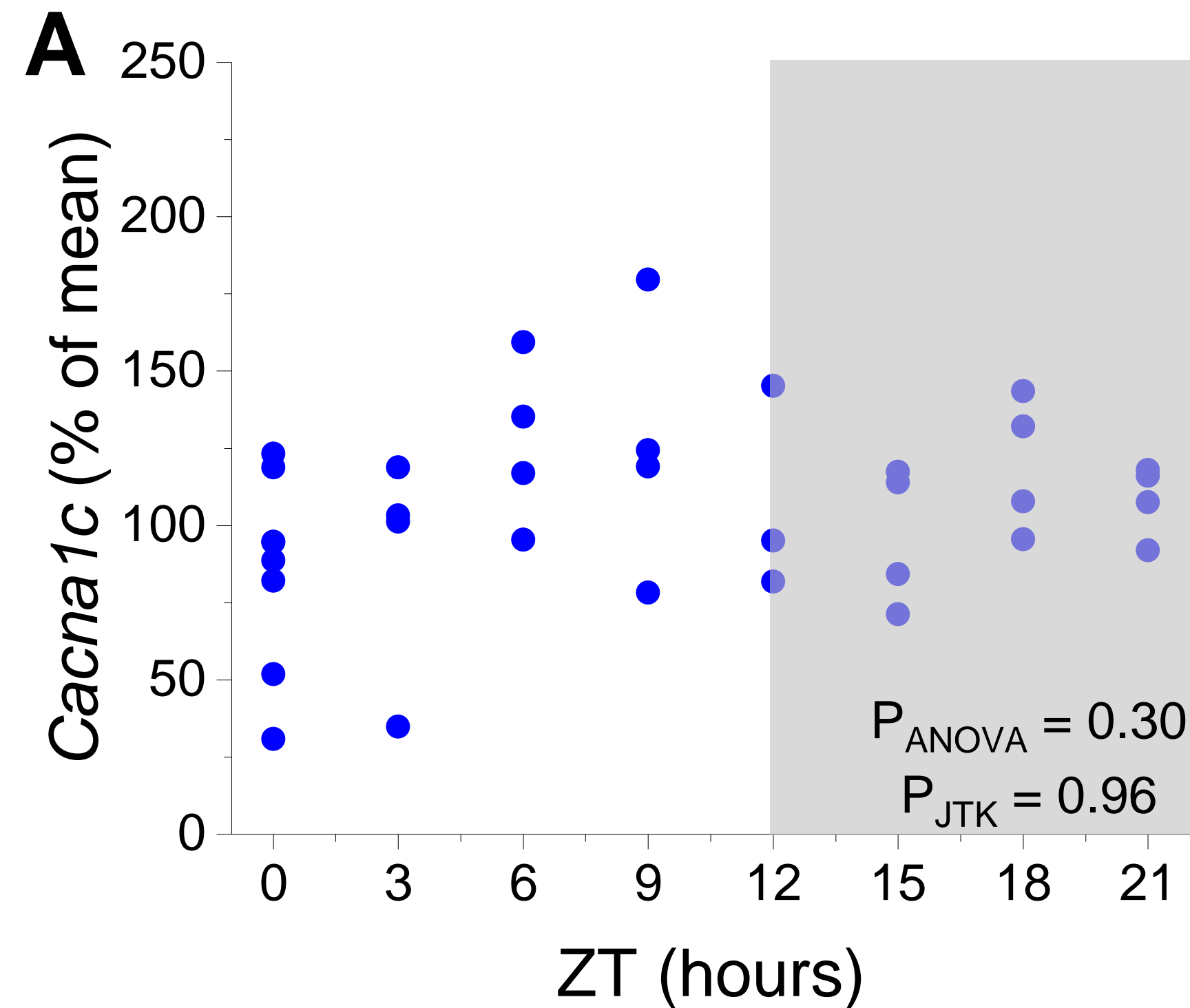


C

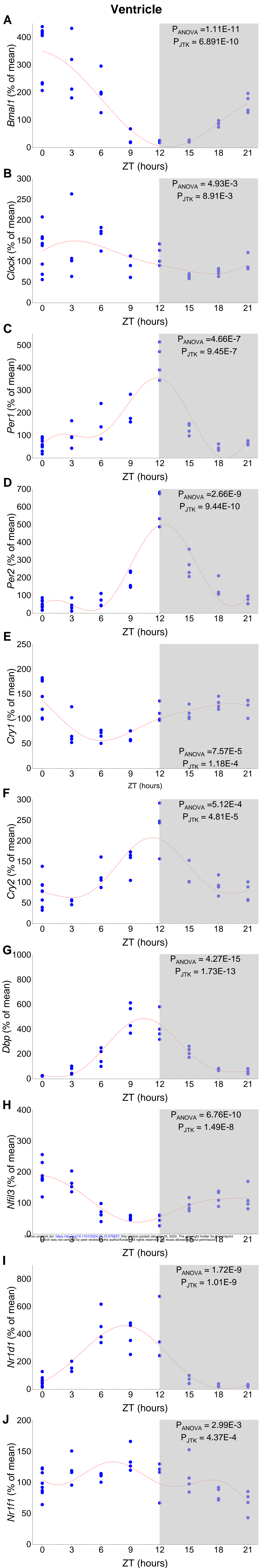


D

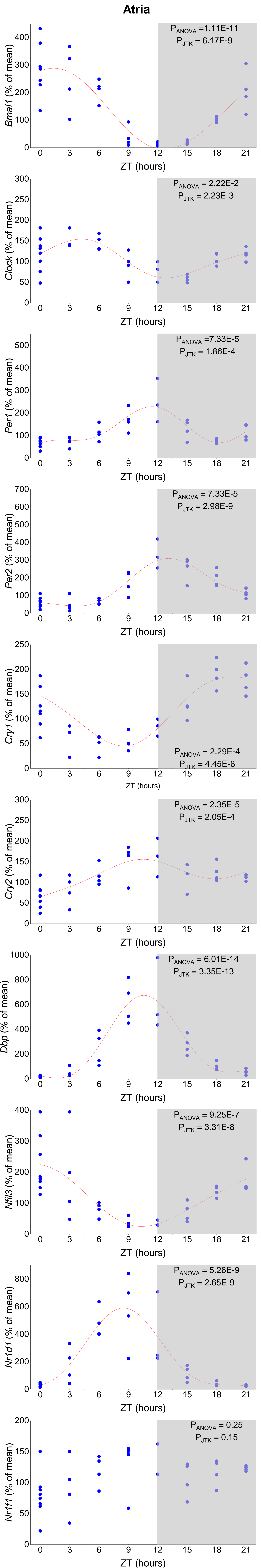


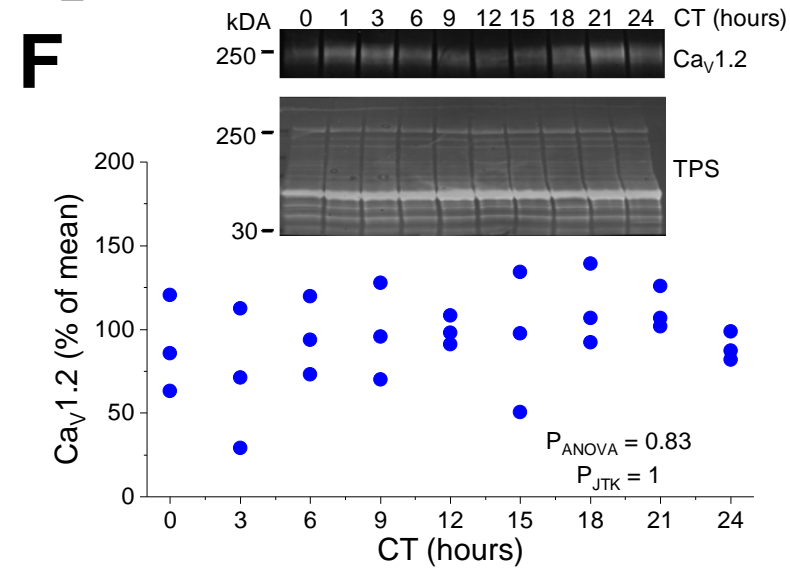
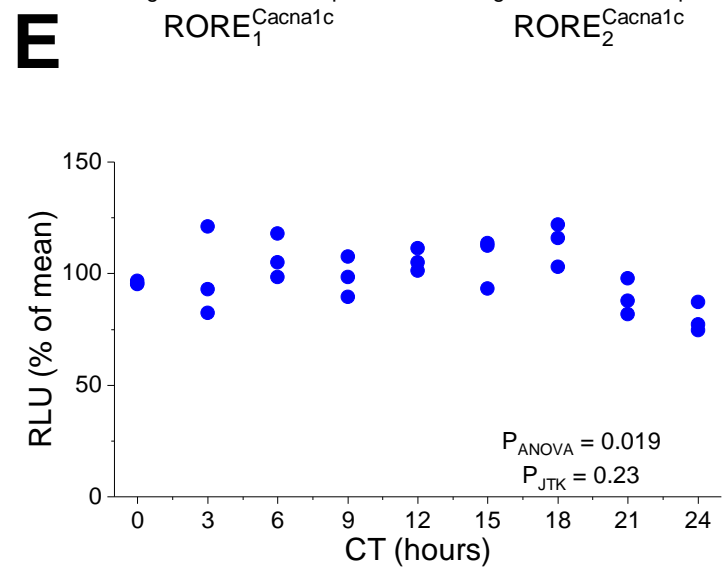
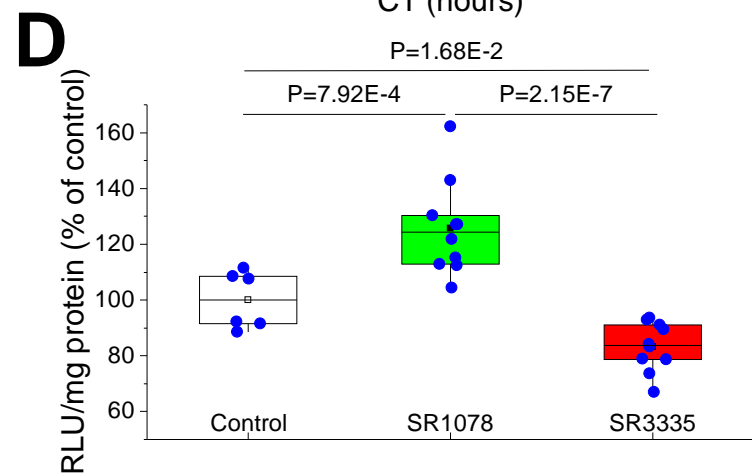
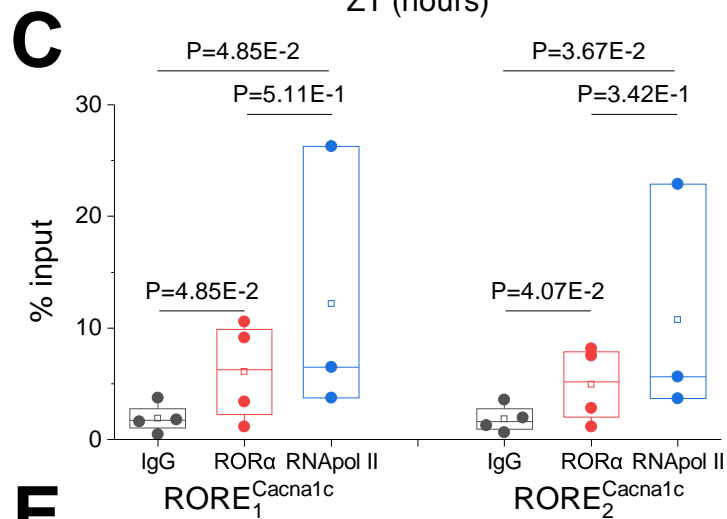
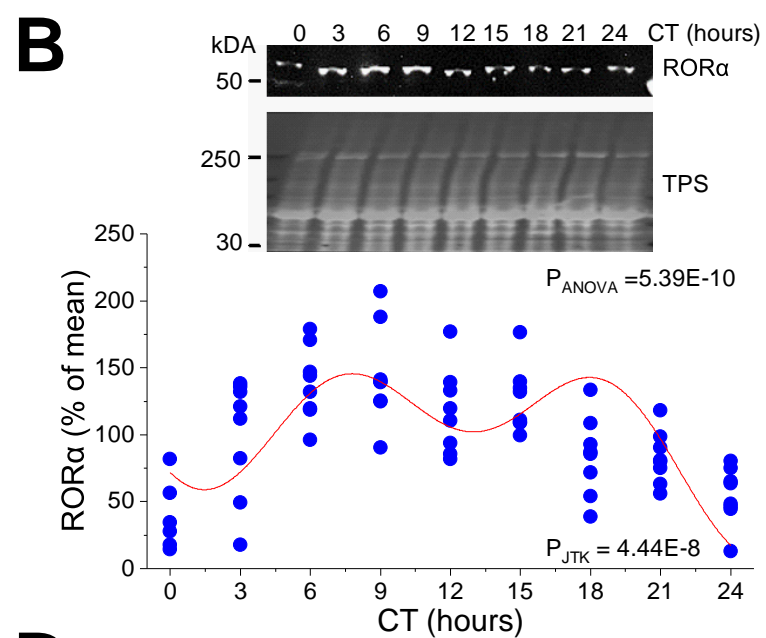
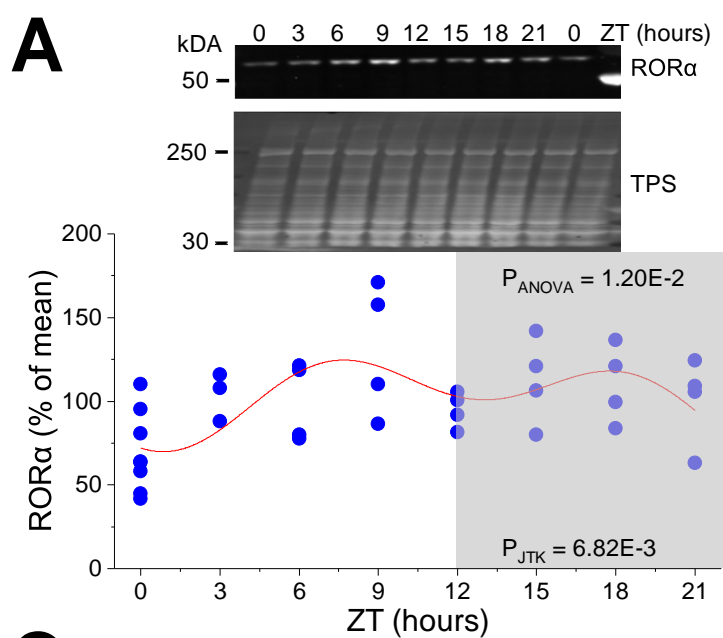


Ventricle



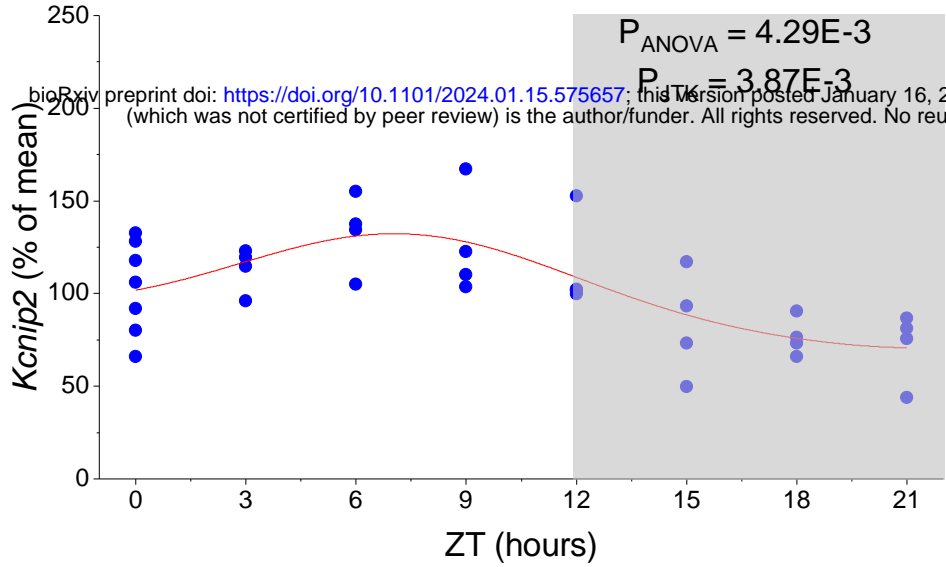
Atria



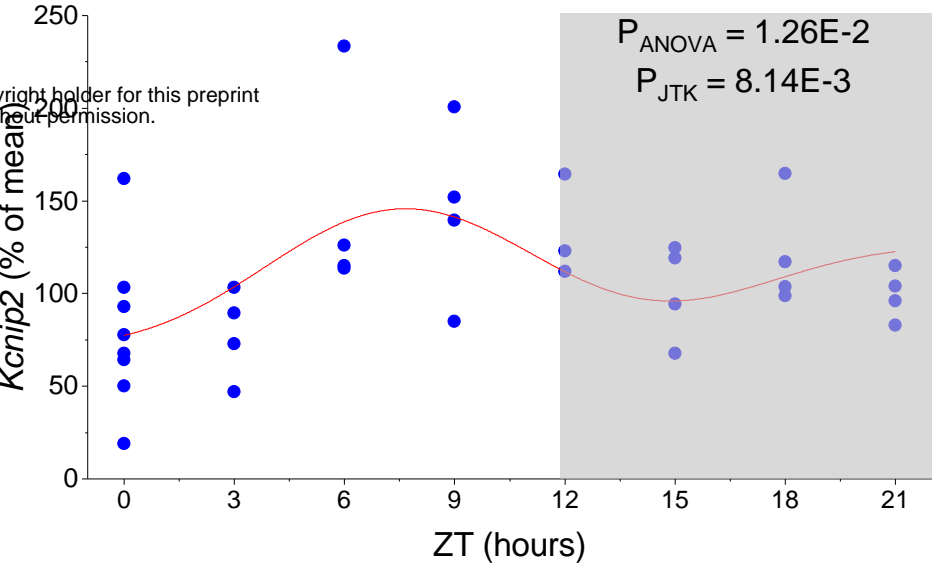


A

Ventricle

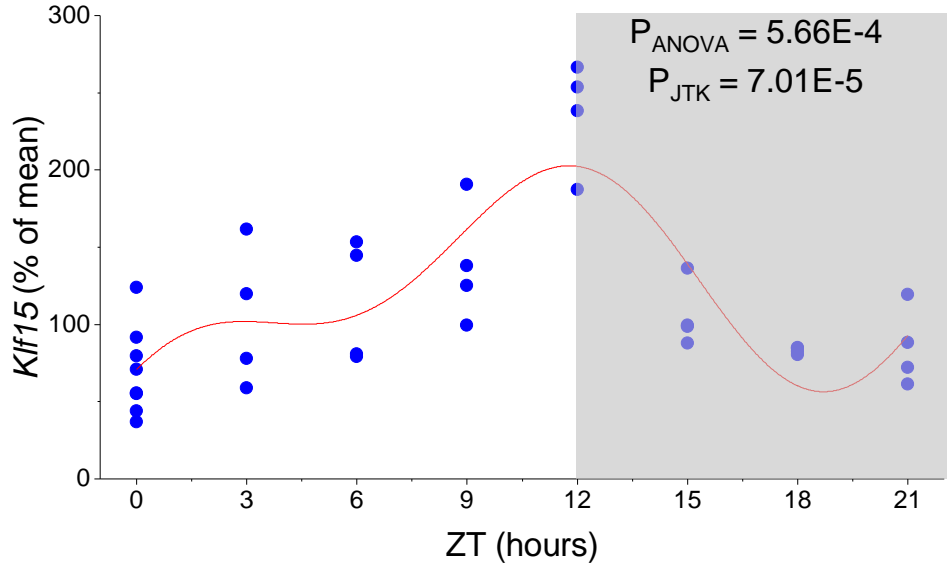


Atria

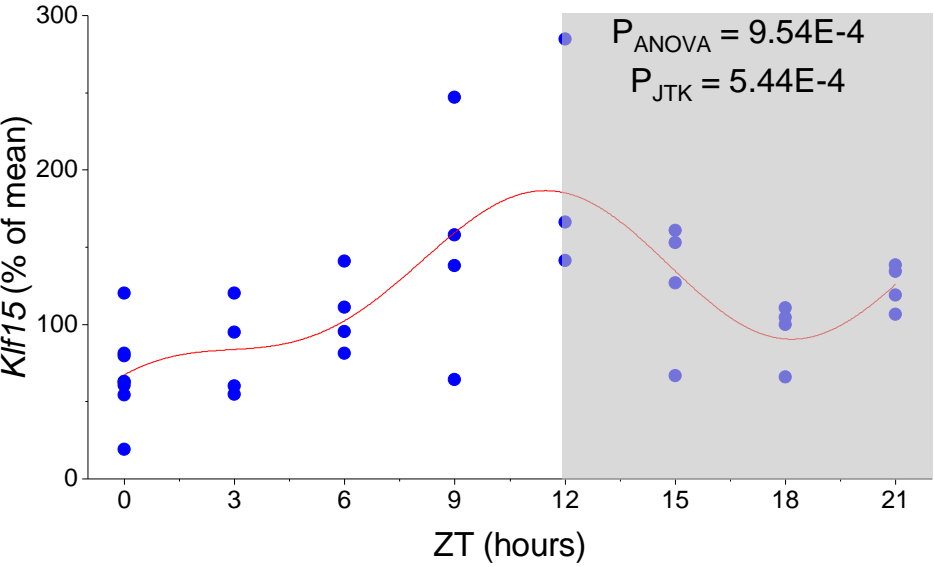


B

Ventricle

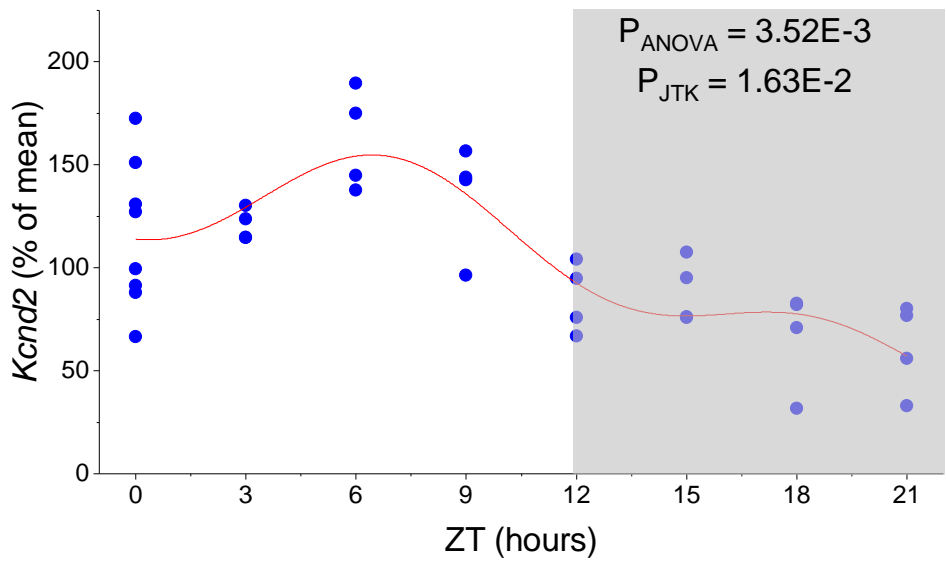


Atria

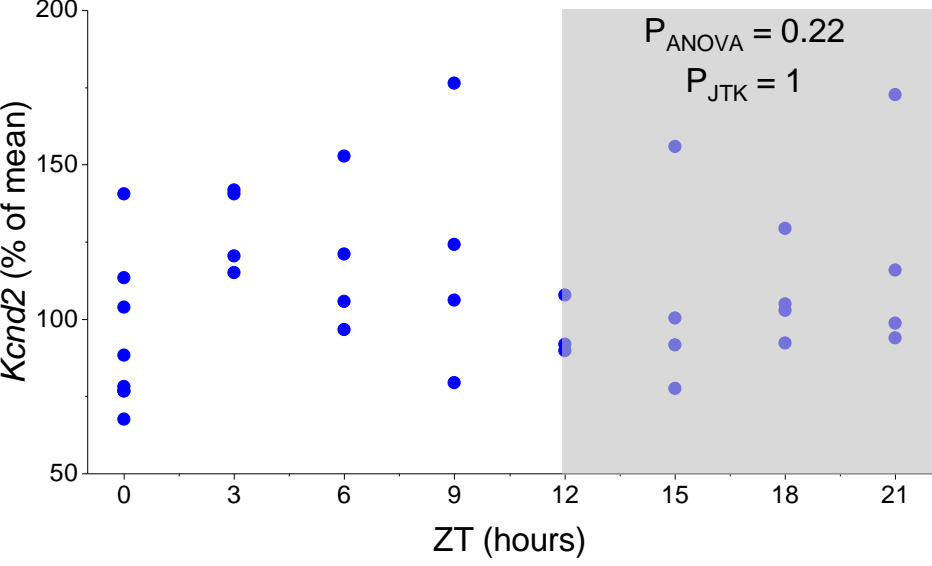


C

Ventricle

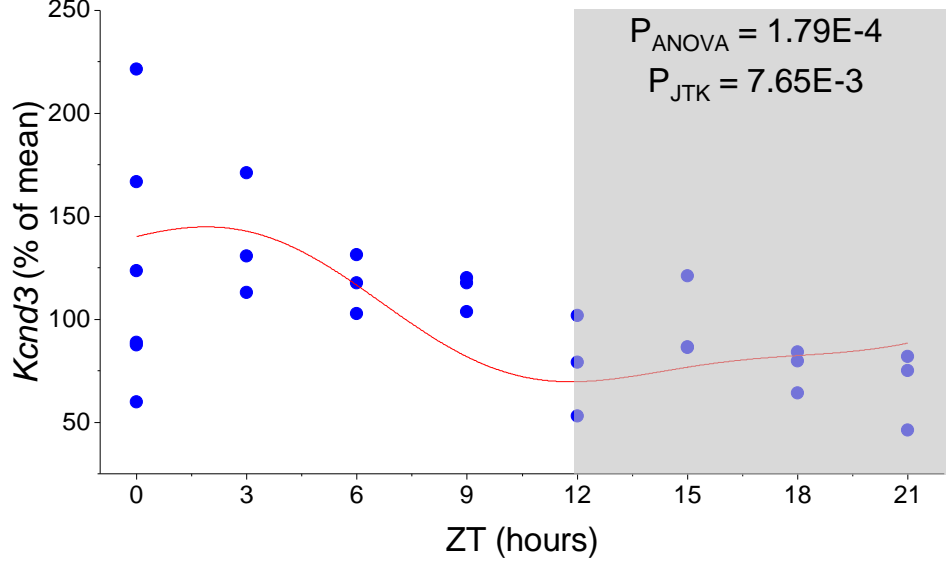


Atria

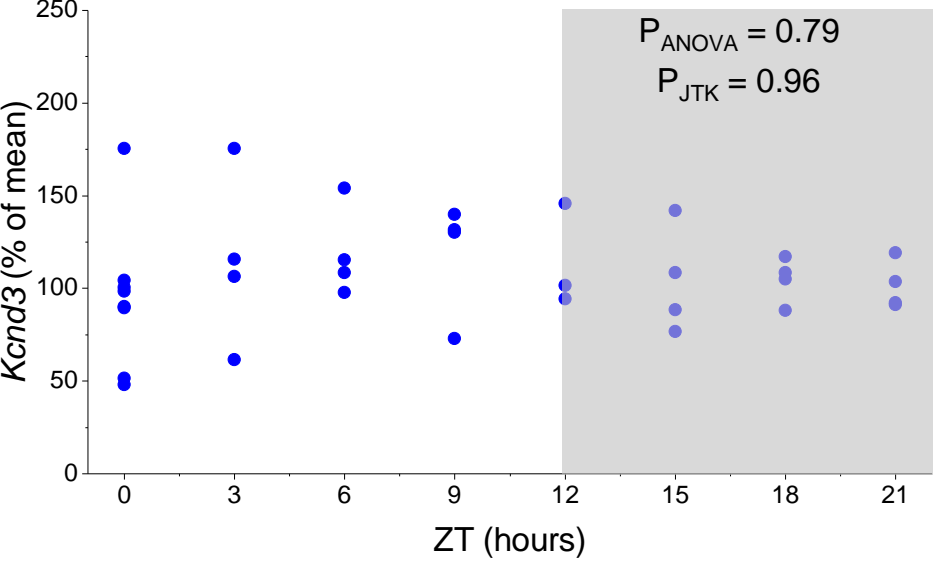


D

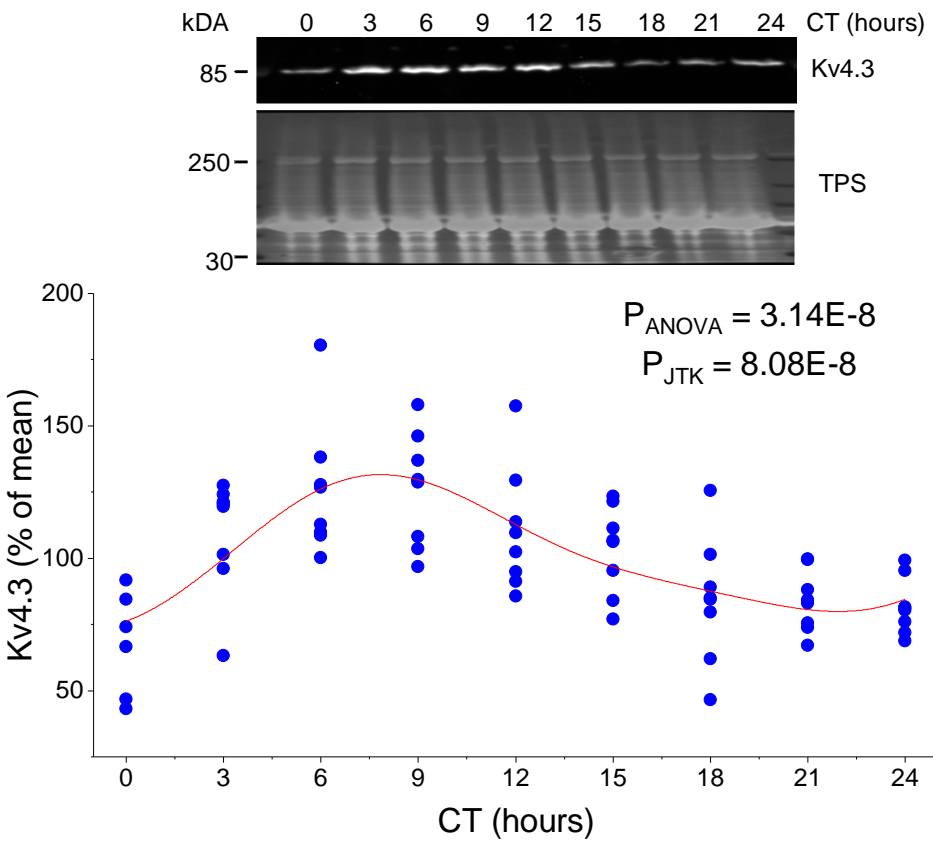
Ventricle



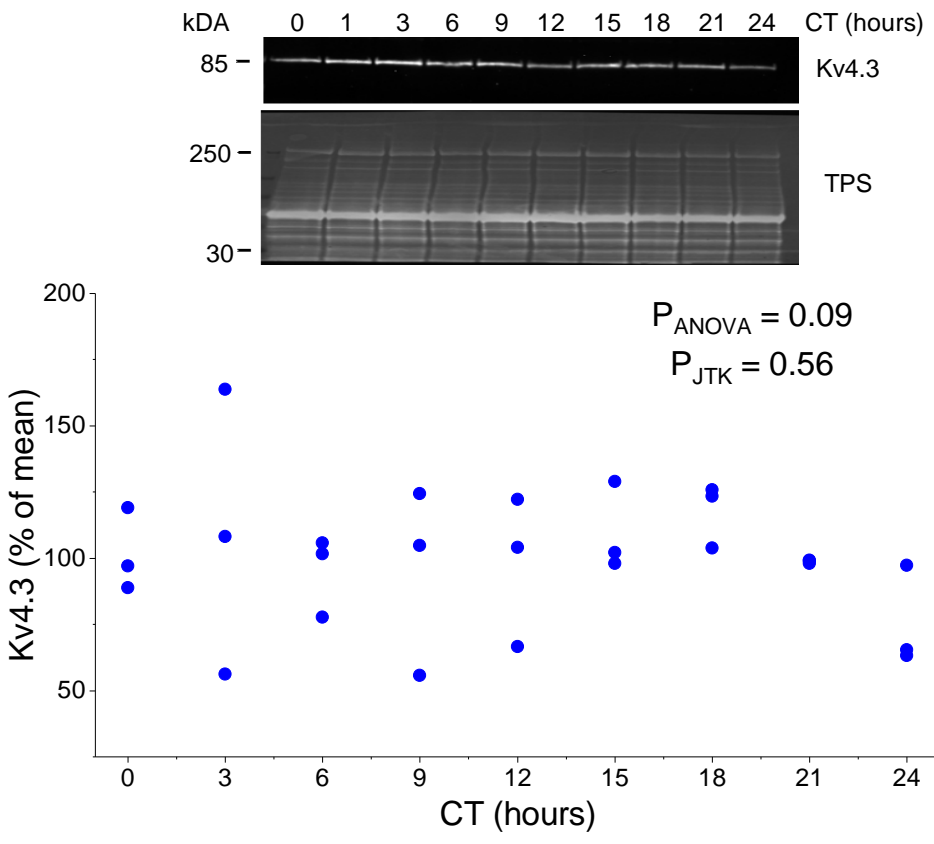
Atria



E



F



G

